

INAUGURAL - DISSERTATION
zur
Erlangung der Doktorwürde
der
Naturwissenschaftlich-Mathematischen Gesamtfakultät
der
Ruprecht-Karls-Universität
Heidelberg

vorgelegt von
Margarita Koroleva
aus Moskau, Russland
Diplom Geologie-Hydrogeologie Fachbereich „Hydrogeologie und
Ingenieurgeologie“ Moskauer Staatliche Lomonosov-Universität
Magister der Geologie Moskauer Staatliche Lomonosov-Universität

Tag der mündlichen Prüfung: 13.06.2005

Thema:

**Basic studies for the incorporation of uranium in
sediments**

Gutachter:

**Prof. Dr. Augusto Mangini
Prof. Dr. Margot Isenbeck-Schröter**

Abstract

Uranium migration in natural aqueous systems is an ongoing concern in environmental research.

Investigation on sorption interactions with soil, sediments and rocks are important to understand uranium mobility, in order to correct U/Th dating methods in open systems.

Uranium immobilization is possible due to reduction U(VI) to U(IV), adsorption or co-precipitation.

Under oxidizing environmental conditions, uranium typically occurs in the hexavalent form as the mobile, aqueous uranyl ion (UO_2^{2+}). Moreover, depending from environmental conditions, uranium forms carbonate complex such as $\text{UO}_2(\text{CO}_3)_2^{2-}$ or $\text{UO}_2(\text{CO}_3)_3^{4-}$.

Uptake of such dissolved metal contaminants by many fine-grained mineral phases (clays, oxides, and hydroxides) is most commonly achieved by adsorption. For carbonates recent evidence suggests that incorporation into solids (co-precipitation) dominant uptake.

Uranium sorption experiments were carried out with lake sediment and aragonite samples. All experiments were conducted using the uranium isotope ^{232}U under ambient pressure and room temperature at different pH.

Sediment samples were obtained from an artificial lake (Willersinnweiher, SW Germany). This lake has relatively high uranium concentration in water and sediment columns. The lake has two seasonally different redox conditions in the water column, which were simulated in the lab. To understand uranium behaviour an artificial uranium isotope was added into the water column. The experiments were conducted at ambient pressure and room temperature. After reaction time the uranium concentration was measured in the water column, in pore water and in sediment column. The results indicate in both cases 80 % of uranium saturated into the sediments. But in oxygenated water uranium penetrated deeper into the sediment.

Adsorption experiments show that adsorption of uranium by the lake sediment is strongly pH dependent, and that adsorption at low and high pH is minimal; the maximum adsorption occurs near neutral pH.

The experiments of uranium uptake by aragonite powder were conducted at pH range 6-11. These experiments show also the strongly pH dependence and maximum of uranium uptake is at pH 7 (98%).

Also experiments regarding (1) the influence of major seawater elements on uranium uptake, (2) uranium transport and (3) kinetic of uranium uptake by aragonite were conducted. Uranium uptake by powdered aragonite is fast (less than 0.3 hours). The content of Mg^{2+} in solution highly decreases the process of uranium incorporation.

Numerical modeling of the process of U(VI) sorption by sediment was conducted. This study shows that the surface complexation model DLM can predict the major three types of uranium behaviours: (1) the increase of uranium adsorption at pH range between 5 and 6.5, (2) the maximum of adsorption at nearly neutral pH and (3) the decrease of uranium adsorption between pH 8 and 11.

Zusammenfassung

Die Mobilität von Uran in der Natur ist von anhaltender Bedeutung in der Umweltforschung.

Eine Untersuchung von Sorptionswechselwirkungen mit Böden, Lockersedimenten und Festgesteinen sind zwingend notwendig, um Uranmobilität besser zu verstehen. Nicht zuletzt für die Korrektur von U/Th Datierungen in offenen Systemen ist dies von großer Wichtigkeit.

Die Immobilisierung von Uran wird ermöglicht durch Reduktion von U(VI) zu U(IV), durch Adsorption oder durch Niederschlag.

Im oxidierenden Umweltmilieu kommt Uran normalerweise als hexavalente Form in dem gelösten mobilen Uranyl-Ion (UO_2^{2+}) vor. Außerdem kann Uran auch Karbonatkomplexe wie $\text{UO}_2(\text{CO}_3)_2^{2-}$ und $\text{UO}_2(\text{CO}_3)_3^{4-}$ bilden, in Abhängigkeit von den Umweltbedingungen.

Die Aufnahme dieser gelösten metallischen Verunreinigungen durch feine Mineralphasen (Tone, Oxide und Hydroxide) geht meistens durch Adsorption von statten. Bei Karbonaten ist laut jüngster Ergebnisse die Einlagerung in Feststoffe der dominante Aufnahmeprozess (Niederschlag).

Experimente zum Uranverhalten in limnischen Lockersedimenten und in Aragonit wurden durchgeführt. Die Experimente fanden in Raumtemperatur unter Umgebungsdruck bei verschiedenen pH-Bedingungen statt.

Die Sedimente eines künstlichen Sees (Willersinnweiher, SW Germany) wurden beprobt. Dieser See hat eine relativ hohe Urankonzentration in Wasser und Sediment. Zwei jahreszeitlich verschiedenen Redoxbedingungen der Wassersäule wurden im Labor simuliert. Nach Zugabe des künstlichen Uranisotops ^{232}U in die Wassersäule wurde nach einer bestimmten Reaktionszeit die Konzentration jeweils in der Wassersäule, im Porenwasser und im Sedimentpaket gemessen. Das Resultat ist unter beiden Redoxbedingungen eine 80% Uransättigung im Sediment. Jedoch dringt Uran im sauerstoffreichen Wasser tiefer in das Sediment ein.

Die Adsorption von Uran durch Seesedimente ist stark von der pH-Bedingung abhängig. Maximale Adsorption läuft bei annähernd neutralem pH ab, während geringe Adsorption bei hohen und tiefen pH-Werten stattfindet.

Experimente zur Uranaufnahme von Aragonitpulver wurden im pH-Bereich von 6 bis 11 durchgeführt. Hier wurde ebenfalls eine starke pH-Abhängigkeit nachgewiesen, mit einer maximalen Aufnahme von 98% bei pH 7.

Ebenso wurden Experimente bezüglich (1) des Einflusses wichtiger Meerwasser-elemente auf die Uranaufnahme, (2) Transport von Uran und (3) Kinetik der Uranaufnahme durch Aragonit durchgeführt. Ergebnisse sind, dass Uranaufnahme in Aragonitpulver schnell abläuft (in weniger als 0,3 Stunden), und dass der Gehalt von gelöstem Mg^{2+} den Prozess der Uraneinarbeitung beträchtlich herabsetzt.

Eine numerische Modellierung der U(VI)-Sorptions durch Sedimente wurde durchgeführt. Mit dem Oberflächen-Komplexbildungs-Modell ist eine Voraussage der drei wichtigen Verhaltensweisen von Uranadsorption möglich: (1) den Anstieg der Uranadsorption zwischen pH 5 bis 6,5, (2) das Adsorptionsmaximum bei nahezu neutralem pH-Wert und (3) der Adsorptionsabfall zwischen pH 8 und 11.

TABLE OF CONTENTS

<i>Introduction</i>	3
<i>Chapter 1. Literature review and purposes of research</i>	5
1.1. Uranium in the natural environment	5
1.1.1 Uranium thermodynamics.....	6
1.1.2. Reducing environments	6
1.1.3. Oxidizing environments.....	7
1.1.4. Transport of U in river water.	7
1.1.5. Uranium interaction with minerals	8
1.2. A model of the Uranium adsorption	9
1.2.1. Surface complexation models	10
1.2.1.1. <i>Interface (electrostatic sorption) models</i>	11
1.3. Uranium carbonate complex	15
1.4. Purposes of research	18
<i>Chapter 2. Objects of research and sample characteristics</i>	19
2.1. Lake Willersinnweiher.....	19
2.1.1. Temperature layers and water circulation	21
2.1.2. Uranium in the water column.....	23
2.1.3. Lake sediment	25
2.1.3.1. <i>Uranium concentration in the sediment column</i>	26
2.1.3.2. <i>Sediment sample characteristics</i>	27
2.2. Calcium carbonate samples.....	27
<i>Chapter 3. Methods</i>	29
3.1. Sampling	29
3.2. Preparation of samples.....	29
3.3. Investigation of samples	30
3.4. Uranium determination	31
3.4.1. Radiochemical procedure.....	31
3.4.2. Alpha-spectrometry.....	31
3.5. Laboratory experiments.	33

TABLE OF CONTENTS

3.5.1. Laboratory simulation of redox conditions	33
3.5.2. Sorption experiments	33
3.5.2.1. <i>Sample preparation</i>	34
3.5.2.1.1. Lake sediment.....	34
3.5.2.1.2. Calcium carbonate.....	35
3.5.2.2. <i>Experimental procedure</i>	36
3.5.3. Desorption.....	36
3.5.3. Column experiment.....	37
<i>Chapter 4. Results & Discussion</i>	39
4.1. Redox simulation	39
4.2. Lake sediment.....	41
4.2.1. Uranium (VI) adsorption at pH range between 2-11.....	41
4.2.2 Desorption.....	46
4.2.2.1. <i>Desorption at pH range 2–11</i>	46
4.2.3. Adsorption at pH 7.....	47
4.2.4. Summary.....	49
4.3. Uranium uptake by calcium carbonate.....	49
4.3.1. pH influence on U(VI) uptake	49
4.3.2. Uranium uptake at pH 7.....	50
4.3.2.1. <i>Kinetic experiment</i>	51
4.3.2.2. <i>Influence of solution compound</i>	52
4.3.2.3. <i>Transport experiment</i>	53
4.3.3. Summary.....	54
<i>Chapter 5. Model of the uranium adsorption process onto the sediment surface</i>	55
5.1. Modelling.....	55
5.2. Summary.....	64
<i>Conclusions</i>	65
<i>REFERENCES</i>	67

Introduction

Uranium migration in natural aqueous systems is an ongoing concern in environmental research. Sorption interactions with soils, sediments and rocks are important mechanisms for understanding the uranium mobility in natural environment and correction of U/Th dating methods for open systems.

Uranium immobilization is possible due to reduction U(VI) to U(IV), adsorption or co-precipitation. Under oxidizing environmental conditions, uranium typically occurs in the hexavalent form as the mobile, aqueous uranyl ion (UO_2^{2+})[66]. Uptake of such dissolved metal contaminants by many fine-grained mineral phases (clays, oxides, and hydroxides) is most commonly achieved by adsorption. pH of solution is a key parameter, which controls the process of uranium adsorption.

Adsorption of dilute solutes onto immobile solids is a key process for retarding the movement of solutes with groundwater flow. The imbalance of forces at phase boundaries drives such adsorption reactions. Ions in an aqueous electrolyte will migrate to charged surfaces such as clay minerals. Non-polar solutes such as hydrocarbons will displace water molecules at a non-polar surface such as sedimentary carbon. Dissolved metal ions and ligands will respectively bind to functional groups and metal centres on organic or mineral surfaces, analogous to hydrolysis and complexation reactions in solution.

Moreover, depending from environmental conditions, uranium forms a carbonate complex such as $\text{UO}_2(\text{CO}_3)_2^{2-}$ or $\text{UO}_2(\text{CO}_3)_3^{4-}$ [20].

For calcium carbonates, recent evidence suggests that uranium incorporation into the solid phase (co-precipitation) is the dominant uptake [55]. Structural incorporation of U into calcium carbonate minerals is depending on environmental conditions (U/Ca) [40]. Formation of U(VI) aqueous carbonate-complexes, which appear to be nonsorbing reduces the activity of UO_2^{2+} and drives the reaction in the opposite direction (decreasing sorption)[52].

Enrichment of uranium is the basic requirement of U/Th dating of rocks. Determination of absolute age is based on the fact that a given radionuclide decays at a known rate, and forms a *geological clock* [36]. Nuclear dating methods are based upon the assumption that systems have been closed to isotopic exchange. The fundamental criterion for datability of any sample is that the sample remains closed to nuclide migration from the time of formation to the time of measurement. The measured age is then that of the last opening event. However, reliable ages are difficult to obtain because many geological systems evolve in an open system with respect to most radioactive nuclides. There are many different models, which help to apply U/Th dating method to open system. In order to upgrade these models it is necessary to know radionuclide migration in the nature.

Introduction

The objectives of this thesis are uranium sorption experiments, which were carried out with lake sediment and aragonite samples.

In the first chapter the uranium behaviour in the natural environment and model of uranium sorption process are discussed. The purposes of this research are described here too.

The second chapter describes the two objects of research. The first is an artificial lake, Lake Willersinnweiher in SW Germany. Natural conditions and physical- chemical characteristics of the lake sediments and natural uranium concentrations in the water and sediment columns are discussed there. The second object is fossil coral samples from Barbados.

In chapter three the methods of sampling, uranium determination and sorption experiments are described.

Chapter four is dedicated to results and discussions of the laboratory experiments.

Chapter five displays a thermodynamic model based on a surface complexation approach for prediction of U(VI) sorption.

This research was carried out within the framework of the Graduiertenkolleg 273, which was funded by the Deutsche Forschungsgemeinschaft (DFG).

Chapter 1. Literature review and purposes of research

1.1. Uranium in the natural environment

Usually uranium concentration of the continental crust range from $0.1 \mu\text{gg}^{-1}$ (basalt) to $6 \mu\text{gg}^{-1}$ (granite), in limestone formations are $\sim 2 \mu\text{gg}^{-1}$ and up to $\sim 10 \mu\text{gg}^{-1}$ in speleothems (Ivanovich and Harmon, 1992) [36].

The naturally occurring uranium isotopes U^{238} , U^{235} , U^{234} are dissolved during chemical weathering and form the stable uranyl species in oxidizing aqueous environments (pH approximately 6 or greater, Langmuir (1978)). In suboxic to anoxic environments, particularly marine sediments, hexavalent uranium can be reduced to tetravalent uranium and removed from solution.

Nuclear dating methods are based upon the assumption that systems have been closed to isotopic exchange. The measured age is then that of the last opening event. However, reliable ages are difficult to obtain because many geological systems evolve in an open system with respect to most radioactive nuclides. The dating methods based on U-series disequilibrium are particularly sensitive to diagenesis and alteration, which generate large chemical (e.g. U-Th-Ra-Rn-Pb) and even isotopic (e.g. ^{234}U - ^{238}U) fractionations. Isotopic fractionations are favoured by the large spectrum of geochemical behaviour displayed by elements inside the uranium series and by the large energies released by radioactive decay. The latter induce destabilisation of radioactive daughters in host material (e.g. lattice damage, K-recoil, decay-related oxidation).

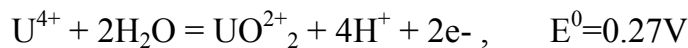
These effects are time dependent and the probability that a system opens, increases with time. The ^{238}U - ^{234}U - ^{230}Th method is largely used for dating recent events (i.e. 350 ka) in numerous domains of geological and environmental sciences and is particularly suitable for sedimentary material (Villemant and Feuillet, 2003) [72].

1.1.1 Uranium thermodynamics

During weathering processes and transfers into river-waters, fraction among nuclides of different chemical elements are largely controlled by the differences in chemical properties of these elements in solution. The properties are controlled by the classical thermodynamic parameters of aqueous solutions: temperature, pressure and solution composition (pH, redox potential, ionic strength and occurrence of complex forming ligands). The thermodynamic properties of actinides in aqueous solutions have been studied by: Grenthe et al. (1992), Langmuir (1997) [9].

Uranium thermodynamic data indicate that in environmental conditions the predominant species stable with H₂O are in either U(IV) or U(VI) oxidation state.

Under reducing conditions, U(IV) is very insoluble and tends to participate as insoluble uraninite. In the IV oxidation state uranium is almost chemically immobile in the near-surface environment at low temperatures. However, uranium may be mobilized by oxidation to the VI state (Langmuir, 1979):



Further complexing of the uranyl ion may then occur depending on pH and presence of the other ions [9].

1.1.2. Reducing environments

Only uranous (IV) species having appreciable solubility in natural water are fluoride and hydroxyl complexes at low Eh conditions [36]. In pure solutions, under reducing conditions, U(IV) forms hydroxy complexes:



Where $0 \leq n \leq 5$, and n is dependent largely on temperature and pH [9].

UO_{2(s)} solubility is largely independent of water chemistry (fluoride complexes only become significant below pH 4), temperature (between 25 and 300°C) and pH ($4 < \text{pH} < 10$). The dissolved U(IV) species is predominantly U(OH)₄ and the solubility of uranium is $\sim 10^{-9.5}$ M (or about 0.06 ppb) [36].

1.1.3. Oxidizing environments

In oxic conditions uranyl complexes are far more soluble than uranous species, U is under its most oxidized state U(VI), which forms in aqueous environments the linear uranyl ion UO_2^{2+} , easily complexes with carbonate and hydroxide, and also with phosphate, fluoride and silicate ions [9]. Uranyl (UO_2^{2+}) is typically the predominant free aqueous species in natural water systems under aerobic, acidic conditions ($\text{pH} < 5$) (J.S.Arey et al 1999). The dominating species in water will depend on Eh- pH conditions, the concentration and availability of complexing ions and temperature. Uranium (VI) is considerably more soluble than U(IV) and the formation of uranyl complexes, such as carbonate and phosphate complexes, significantly increases the solubility of U minerals and the mobility of U in surface and groundwater. U(VI) also forms stable complexes with dissolved organic carbon (DOC) [9]. Li et al. 1980 measured stability adsorption constants for U(VI) with fulvic acid, humic acid, and tannic acid on the order of 10^7 at “strong” binding sites and 10^5 at “weak” binding sites. The affinity of these organics for U drops dramatically as pH falls below 5, depending on the ligand (J.S.Arey et al., 1999).

1.1.4. Transport of U in river water

The transport of U in fractured bedrock by oxidizing waters is an important process in the cycling of this element from the geosphere to the biosphere [9]. In U rich systems, such as natural U deposits and U tailings, the dissolution process typically involves oxidation and destabilization of U(IV) minerals such as uranite (UO_{2+x}) and coffinite ($\text{USiO}_4 \cdot n\text{H}_2\text{O}$) resulting in high concentrations of U(VI) aqueous species. In these types of environments U concentrations may reach values higher than 10,000 mg/L (Miekeley et al., 1992; Langmuir, 1997; Jerden Jr. And Sinha, 2002)

Adsorption and precipitation reactions are controlled in large part by the compositions of groundwater, which often contain natural and anthropogenic (contaminant) U(VI)-complexing ligands such as carbonate, phosphate, citrate, NTA, and EDTA. Many competing reactions can occur between U(VI), Fe-oxide surfaces, and ligands, including U(VI) adsorption on Fe-oxides, ligand adsorption, aqueous complexation of U(VI) ions by ligands, adsorption of U(VI)-ligand complexes (ternary complex formation), ligand-promoted dissolution of Fe(III) from Fe-oxides, and re-adsorption of Fe(III)-ligand complexes [2,7,9,18,36,49,50]. Definition of such reactions and of the identities (*i.e.*, structures and compositions) of major source-sink species is necessary to the development of accurate

predictive models of uranium fate and transport in subsurface environments of widely varying chemical conditions. Such models are used to assess risk to humans and wildlife at contaminated sites and to make policy decisions. Such knowledge is also essential to the design of remediation technologies that rely upon long-term stabilization of U(VI) in the subsurface (e.g., in-situ techniques) or upon enhanced extraction of U(VI) from the subsurface (e.g., pump-and-treat). Furthermore, since actinide-bearing mixed wastes commonly contain hydrous metal oxides and chelating ligands, knowledge of metal-ligand-oxide interactions is also relevant to the design of effective separations procedures [9].

In surface waters, which are nearly always oxygenated, U occurs in its soluble form, i.e., U(VI). Uranium often forms complexes with carbonates such as $\text{UO}_2(\text{CO}_3)_2^{2-}$ or $\text{UO}_2(\text{CO}_3)_3^{4-}$ and with phosphate. A significant proportion of U in rivers is transported as suspended particles, recovered by filtration at 0.1-0.45 μm . The complexation of U by organic colloids is greater for humic acids than for fulvic ones (Lenhart et al., 2000) and pH-dependent (Read et al., 1993, Lienert et al., 1994). In organic-rich water, up to 75-90% of “dissolved” U can be in a colloidal form (Viers et al., 1997; Dupré et al., 1999).

1.1.5. Uranium interaction with minerals

The transport of U(VI) in soils and aquifers is strongly affected by sorption on mineral surfaces and precipitation reactions involving groundwater solutes. The adsorption of U onto mineral surface is so important that it can become a limiting factor for the mobility of U in surface and groundwater [9]. Uranium sorption onto different mineral surface was studied by Barnett et al. (2000, 2002), Arnold et al. (1998), Echevarria et al. (2001), Missana et al. (2003), Pabalan and Turner (1997).

Sorption is the attraction and adhesion of ions from an aqueous solution to a solid with which it is in contact.

Among the parameters that control the elemental adsorption onto mineral surfaces are physical parameters such as temperature, cationic exchange capacity and specific surface area (Borovec 1981; Priklyl et al., 2001), but also chemical characteristics of the solution: pH, ionic strength, organic and inorganic ligand concentrations [9].

Generally, the capacity of U sorption onto mineral surface decreases from Fe-oxides and silica gels, to clays and micas and to opals (e.g., Ames et al. 1983; Allard et al., 1999). Fe-oxides, such as goethite, and ferrihydrite (pseudoamorphous $\text{Fe}_2\text{O}_3 \cdot x\text{H}_2\text{O}$), are frequently implicated as being among the most important inorganic adsorbent phases, and surface waters, their high sorptive capacities for U(VI), and their high surface areas [9].

Pabalan and Turner (1997), Barnett et al. (2002) have shown that U(VI) sorption is strongly sensitive to pH and to formation of aqueous U(VI) carbonate complexes. The major

features of pH-dependent uranium adsorption to mineral surface: the sharp increase in adsorption from pH 3 to pH 5 (i.e., the “first” pH adsorption edge), the plateau in adsorption from pH 5 to pH 8, and the dramatic decrease in adsorption from pH 8 to pH 9 (i.e., the “second” pH adsorption edge) [6, 7, 52].

Bargar et al. (1999) have shown that uranium mobility in aquifers may be controlled by adsorption of U(VI)-carbonate complexes on oxide minerals. In this research U(VI)-carbonate complexes were found to be the predominant adsorbed U(VI) species at all pH values examined, a much wider pH range than previously postulated based on analogy to aqueous U(VI)-carbonate complexes, which are trace constituents at pH < 6 [4].

The uranium sorption on a solid phase can be quantitatively described by the *distribution coefficient (K_d)*, *adsorption isotherms*, and *surface complexation models*. The K_d is simply the result of an experimental measurement in a closed system, which a known amount of solid and a certain volume of a solution of known composition resides. Surface complexation models aim to specify the sorption process of aqueous ions on a solid phase. The models are based on the assumption that sorption takes place via chemical reaction between the aqueous species and specific surface binding sites. Hereby, sorption is distinguished in chemical bonding of the on aqueous ion with the surface site, i.e. chemisorption and formation of inner sphere complexes, and physical adsorption, in which the aqueous ion sticks to the surface via electrostatic forces and forms outer sphere complexes.

1.2. A model of the Uranium adsorption

Interactions taking place at phase boundaries, i.e. interaction of trace element and radionuclide species as well as organic components in water with sediments, occur via reversible and irreversible processes.

Reversible surface interactions are usually rapid processes, while the diffusion through double layers into mineral lattices is very slow process. Therefore, the assumption of equilibrium conditions is relevant for reversible processes (physical sorption, electrostatic sorption), but questionable for irreversible (chemisorption) processes. By adding radioactive tracers in cationic form to a seawater-sediment system, the equilibrium between species in solution and species easily mobilised from solid surfaces by an inert electrolyte (Figure 1.1) is established between 2-7 days depending on temperature, while years are needed to establish equilibrium with the irreversible inert phases [10].

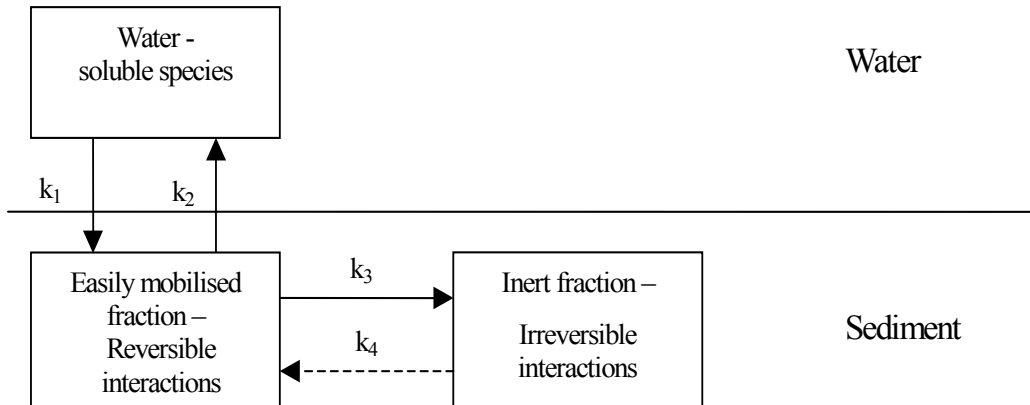


Figure 1.1. Box model dividing the sediment-water system into three operational compartments, which are connected by apparent rate constants, described by first order kinetics. (Peer Børretzen & Brit Salbu, 1999) [10]

1.2.1. Surface complexation models

An alternative to the empirical modelling approaches are the surface complexation models (SCM), which extend the ion-association model of aqueous solution chemistry to include formation of chemical complexes on surfaces. SCMs treat surface functional groups as analogues of complexing ligands in solution. The main difference between the various models lies in the assumed structure of the surface complexes thought to be formed. While the models differ in their consideration of interfacial structure, all the models reduce to a set of simultaneous equations that can be solved numerically (Dzombak et al. 1987). These equations include:

- (1) mass law equations for all surface reactions under consideration,
- (2) a mole balance equation for surface sites,
- (3) an equation for computation of surface charge,
- (4) a set of equations representing the constraints imposed by the model of interfacial structure.

A number of different surface complexation models have been proposed during the last three decades. The models are distinguished by differences in their respective molecular hypotheses. Each model assumes a particular interfacial structure, resulting in the

consideration of various kinds of surface reactions and electrostatic correction factors to mass law equations (Davis & Kent, 1990).

Traditional applications of SCMs have relied on simultaneously adjusting different model-specific parameters to produce the best match to given data set. SCMs typically have a large number of potentially adjustable parameters, this approach is likely to result in a nonunique fit that make comparison between models and between studies difficult. Therefore, recent efforts have focused on developing a “standard” set of model parameters. This has the benefit of limiting the number of adjustable parameters and providing a set of uniform SCM parameters that share common reference values [52].

1.2.1.1. Interface (electrostatic sorption) models

Four very common SCMs are the Constant Capacitance Model (CCM), the Diffuse Layer Model (DLM), the Basic Stern Model (BSM), and the Triple Layer Model (TLM) [10].

Diffuse Layer Model (DLM)

In this model, all surface coordinating anions and cations are assigned to the same layer as H^+ and OH^- , and non-specifically adsorbed counter ions are assigned to the diffuse layer (Figure 1.2). In the so called diffuse layer model, the relationship between surface charge and potential is fixed by electric double layer theory. The finite number of surface sites limits the value of the surface charge to reasonable values regardless of the ionic strength. Dzombak and Morel (1990) used two types of surface sites (high-affinity and low-affinity sites) to improve the DLM fit when varying pH [10, 48].

Assumptions

- (i) all surface complexes are inner sphere complexes
- (ii) no surface complexes are formed with ions in the background electrolyte
- (iii) two planes of charge represents the surface
- (iv) the relationships between surface charges and surface potentials are

$$\psi_0 = \psi_d \tag{1}$$

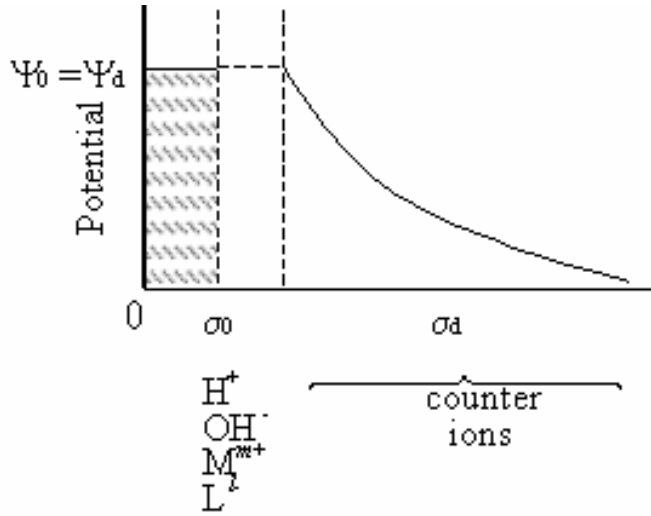


Figure 1.2. Diffuse layer model (Peer Børretzen & Brit Salbu, 1999) [10]

The first layer of charge is located at the oxide surface and produced by the specifically adsorbed ions. A diffuse layer of counter ions, that balance the surface charge, is located in the solution near the solid. The distribution of the ions in the diffuse layer follows the Gouy-Chapman equation.

Gouy-Chapman equation for symmetrical electrolytes

$$\sigma_d = -\frac{Sa}{F} (8\epsilon_0 DRTI)^{1/2} \sinh\left(\frac{\psi_d F}{2RT}\right) \quad (2)$$

or general case

$$\sigma_d = -\frac{Sa}{F} \text{sgn}\psi_d \left\{ 2\epsilon_0 DRT \sum_i c_i [\exp(-z_i F \psi_d / RT) - 1] \right\}^{1/2} \quad (3)$$

where ϵ_0 is the permittivity of vacuum, D is the dielectric constant of water, I is the ionic strength, F is Faraday constant (Cmol_c^{-1}), S is the surface area (m^2g^{-1}), a is the suspension density (gL^{-1}), $\text{sgn}\psi_d = 1$ if $\psi_d > 0$ and $\text{sgn}\psi_d = -1$ if $\psi_d < 0$ (where d represents the diffuse plane), and c_i and z_i are the concentration and charge of solution species i .

A generalised species-component matrix shows the formation of the species from the components for the DLM (Table 1.1).

Table 1.1. Stoichiometry of the equilibrium problem for the double layer model (DLM) (Goldberg, 1995)

Species	Components				
	$\equiv\text{SOH}$	$\exp(-F\psi_d/RT)$	M^{m+}	L^{l-}	H^+
H^+	0	0	0	0	1
OH^-	0	0	0	0	-1
$\equiv\text{SOH}_2^+$	1	1	0	0	1
$\equiv\text{SOH}$	1	0	0	0	0
$\equiv\text{SO}^-$	1	-1	0	0	-1
M^{m+}	0	0	1	0	0
$\equiv\text{SOM}^{(m-1)}$	1	$m-1$	1	0	-1
L^{l-}	0	0	0	1	0
$\equiv\text{SL}^{(l-1)-}$	1	$1-l$	0	1	1
$\equiv\text{SHL}^{(l-2)-}$	1	$2-l$	0	1	2

The reactions at the surface of the oxide mainly involve the amphoteric surface functional groups (SOH) [48, 50]. The pH-dependent charge is determined by the following protonation/deprotonation reactions:



where SOH_2^+ , SOH and SO^- represent the positively charged, neutral and negatively charged surface sites, respectively, and K_{a1} and K_{a2} are the intrinsic equilibrium acidity constants. The mass law equations corresponding to the reactions Eqn. 4 and 5 are:

$$K_{a1} = \frac{(\text{SOH})\{H^+\}}{(\text{SOH}_2^+)} \exp\left(-\frac{F\psi}{RT}\right) \quad (6)$$

$$K_{a2} = \frac{(\text{SO}^-)\{H^+\}}{(\text{SOH})} \exp\left(-\frac{F\psi}{RT}\right) \quad (7)$$

where $\{ \}$ represents the ion activity and $()$ the ion concentrations. Since the activity coefficients for all the surface species are assumed to be equal the activity of these species can be substituted by their concentration $()$. The exponent represents the coulombic term that accounts for the electrostatic effects (Dzombak and Morel, 1990). ψ represents the surface potential, R the molar gas constant, T the absolute temperature (K) and F the Faraday constant.

Specific adsorption of cations at the surface functional groups can be described with reactions of the following type:



with

$$K_c = \frac{(\text{SOM}^{z-1})\{\text{H}^+\}}{(\text{SOH})\{\text{M}^{z+}\}} \exp\left(-\frac{(z-1)F\psi}{RT}\right) \quad (9)$$

for a monodentate binding or



with K_c

$$K_c = \frac{[(\text{SOH})_2\text{M}^{z-2}]\{\text{H}^+\}^2}{(\text{SOH})^2\{\text{M}^{z+}\}} \exp\left(-\frac{(z-2)F\psi}{RT}\right) \quad (11)$$

for bidentate binuclear binding, where the SOH groups interacts independently with the metal ion [48].

Speciation computer codes

There are a number of speciation codes available. Despite the availability of over two dozen codes, only a small number of codes have been used extensively by soil and environmental scientists. Some of the reasons for the wide acceptance of the most commonly used codes are (Mattigod, 1995): (1) ease and flexibility of data input, (2) availability of extensive sets of thermochemical data, (3) ease of addition and modification of code and data, and (4) the capability to model important classes of reactions such as hydrolysis, complexation, dissolution/precipitation, oxidation/reduction, ion exchange and adsorption [10].

1.3. Uranium carbonate complex

The majority of uranium exists as a uranyl carbonate complex and has an overall negative charge.

For carbonates recent evidence suggests that incorporation into the solid (co-precipitation) is the dominant uptake [55, 56]. Consequently, the degree of localized structural disruption around co-precipitated uranyl species bears significantly on the long-term retention of uranium in carbonate minerals, with implications for the potential for uptake and release of uranium IV soil and groundwater environments as well as for the interpretation of uranium age-dating systematic.

Tatsumoto and Goldberg (1959), from the measurement of the uranium content of aragonite precipitated from seawater in the laboratory, showed that the U/Ca ratio in aragonite is approximately the same as the ratio in seawater in which the aragonite has been precipitated [40]. The measurement of the distribution coefficient of uranium between solution and carbonate is only a useful tool for the understanding of the factors controlling the uranium contents of marine calcareous sediments [40].

Kitano and Oomori (1971) have shown that uranyl ions form complexes with carbonate ions in solution, degree of complex formation of uranyl-carbonate increases with increasing precipitation of carbonate due to of the increase in pH value and the concentration

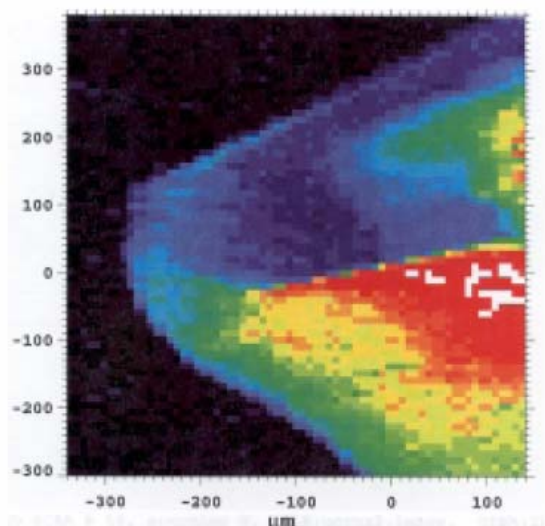


Figure 1.3. Element map over a portion of a calcite 1014 growth face showing total U counts. Highest counts shown in red (Reeder R.J. et al., 2001) [57]

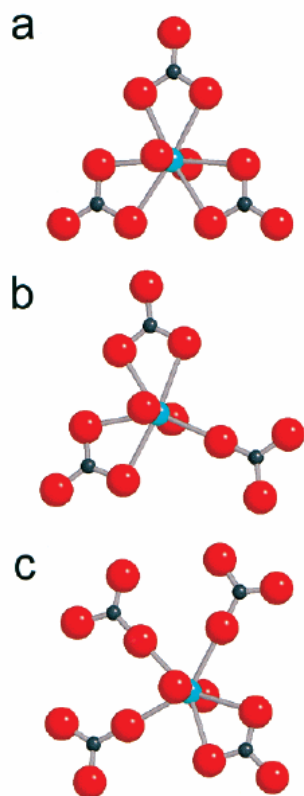


Figure 1.4. (a) Schematic model of the uranyl triscarbonato ion $[\text{UO}_2(\text{CO}_3)_3]^{4-}$, having essentially the same configuration in aqueous solution and as a minor impurity species in aragonite. View shows three CO_3 groups in bidentate coordination in the equatorial plane of the linear $\text{O}=\text{U}=\text{O}$ unit (view slightly displaced from perpendicular to the page). The uranium atom is shown as light blue. (b, c) Possible coordination models of UO_2^{2+} in calcite having five equatorial oxygen atoms in different combinations of monodentate and bidentate coordination. But these observations cannot distinguish between these, and evidence suggests that more than one configuration may occur in the calcite (Reeder et al., 2000) [55]

of CO_3^{2-} although the total amount of dissolved carbonate material decreases [40].

Reeder R.J. et al. (2001) have shown incorporation systematic for the highly mobile uranyl carbonate complexes [e.g., $\text{UO}_2(\text{CO}_3)_3^{4-}$, $\text{UO}_2(\text{CO}_3)_2^{2-}$]. Figure 1.3 shows a representative map of raw uranium counts [57].

Reeder et al. (2000) calculated aqueous speciation for the growth solutions (pH 8.1-8.2) using the Nuclear Energy Agency thermochemical database these data indicate that >97% of the uranium is present as the uranyl triscarbonato complex, $\text{UO}_2(\text{CO}_3)_3^{4-}(\text{aq})$, with 2% as the biscarbonato complex, $\text{UO}_2(\text{CO}_3)_2^{2-}(\text{aq})$.

The structure of the uranyl triscarbonato complex, $\text{UO}_2(\text{CO}_3)_3^{4-}$ consisting of three essentially coplanar CO_3 groups in bidentate coordination in the equatorial plane of the uranyl part (Figure 1.4). Six equatorial oxygens (O_{eq}) are at 2.43 Å, three carbons at 2.88Å, and three distal oxygens at 4.12Å. Reeder et al. (2000) explained it to those that of its

predominance in growth solutions, it is likely that the aqueous uranyl triscarbonato species is primarily involved in the incorporation process during coprecipitation. This same molecular unit, with essentially the same configuration, is almost exclusively adopted by uranyl carbonate compounds. Hence this configuration provides a good starting model for evaluating the local structure of UO_2^{2+} incorporated as a minor component in calcite and aragonite [55, 56].

Incorporation Mechanism. Reeder et al. (2000) have shown that the configuration of the $\text{UO}_2(\text{CO}_3)_3^{4-}$ unit, the dominant aqueous species, is retained by the uranyl in aragonite, suggesting that the entire unit is incorporated into the structure essentially intact. In contrast, a different equatorial coordination occurs in calcite, characterized by fewer nearest oxygens at a closer distance, at least some of which reflect monodentate CO_3 groups, and probably more than one local configuration (i.e., disorder). Hence, the coordination of the UO_2^{2+} unit clearly must change during incorporation into calcite.

Identification of a substitution site for the U(VI) in the carbonate is more problematic than for U(IV) substitution, owing to the size and geometry of the uranyl carbonate complex. The XAFS (x-ray adsorption fine structure) results, which were obtained by Reeder et al. (2002), have shown that, for aragonite sample, 4-5 Ca atoms at a distance 3.8-4.0 Å, with weaker Ca backscattering at 4.75 Å. The aragonite structure has six Ca-Ca distances over the range 3.89-4.10 Å, with four more at 4.7 Å. Hence, U-Ca distances allow an interpretation in which the uranyl triscarbonato complex occupies a portion of the structure corresponding to a Ca polyhedron and some of the coordinated CO_3 groups. But this should not necessarily be interpreted as a substitution of U for Ca, since the aqueous uranyl carbonate species incorporated is an anion and bears no geometrical similarity to Ca^{2+} . For the uranyl-containing calcite, identifying a substitution site is even more difficult. The inability to identify any backscattering from Ca atoms or from O atoms beyond the first equatorial shell from the XAFS of the calcite indicates either a disordered or multiple structural environments for U(VI). The presence of monodentate CO_3 groups would contribute to this disorder because of their greater freedom for tilting and rotation in adapting to the host structure. This disorder in calcite and its apparent absence in aragonite strongly suggests a less stable structural environment for uranyl ion in calcite than in aragonite [55,56].

The XAFS study, which was conducted by Kelly et al. (2003) for U-rich calcite from speleotherm deposit, has shown that uranyl occupies a relatively stable position in the calcite [37].

1.4. Purposes of research

The aim of this work is to study the factors, which have influence on the processes of uranium migration in the natural environment.

Following points of interest are:

- uranium sorption as uranyl ion (UO_2^{2+}) onto mineral surfaces;
- uranium sorption as uranium carbonate complex ($\text{UO}_2(\text{CO}_3)_2^{2-}$ and $\text{UO}_2(\text{CO}_3)_3^{4-}$) onto the sediment surface;
- uranium incorporation as uranium-carbonate complex ($\text{UO}_2(\text{CO}_3)_2^{2-}$ and $\text{UO}_2(\text{CO}_3)_3^{4-}$) into calcium carbonate and factors, which affect the process of incorporation;
- to show differences between U(VI) and U(IV) incorporation;
- to simulate the experimental data with the simplest possible model and to simulate the influence of physico-chemical conditions on uranium sorption behaviour.

Chapter 2. Objects of research and sample characteristics

The first object of the research is lake sediment. The sediment samples were taken from an artificial lake, which has relatively high natural uranium concentration in the water and sediment columns. Natural uranium concentration in the water column is about 0.3 $\mu\text{g/L}$, whereas in the lake sediments it is about 1.6-2.8 $\mu\text{g/L}$. Previous researches (Laukenmann, 2002) have already shown that the main amount of uranium in the sediment column is authigenic.

The second object of the research is calcium carbonate. As literature data already showed, the different mechanisms of uranium immobilization take place in the natural environment. The uranium uptake by calcium carbonate is distinct from the adsorption process, which occurs for lake sediment.

2.1. Lake Willersinnweiher

Lake Willersinnweiher is an artificial lake in south-west Germany, and precisely in the industrial area of Ludwigshafen/Rhein (Figure 2.1). Lake Willersinnweiher began to form in 1930. To the west and south the lake is linked to three other lakes. Morphology of the lake was already provided by Sandler (2000).

Morphologically Lake Willersinnweiher is divided in two basins, a western and an eastern one (Figure 2.2). The maximum depth of the bigger (western) basin is about 20 m; the maximum depth of the smaller (eastern) basin is about 13.5 m. The basins are divided by a dam, which is about 8 m deep. Water volume of Lake

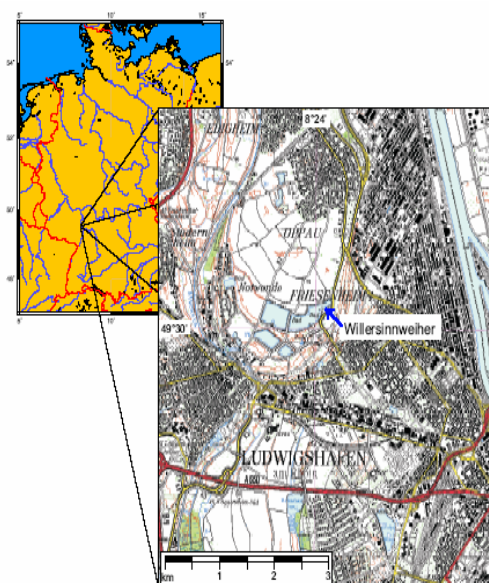


Figure 2.1. Geographical position of Lake Willersinnweiher (Wollschläger, 2003)

Willersinnweiher is about 1.3 million m³, maximum length is 850 m, width is 325 m. The lake has no onground inflow, water input is supplied only by groundwater and by rainfall (about 550 millimeter / year) [77]. The current morphology of Lake Willersinnweiher dates back to 1978. The big basin of the lake showed a maximum depth of about 20 m and the dam, which divided both basins of the lake, was destroyed.

In 1990 sanitary and restoration measures were conducted in order to improve the water quality of Lake Willersinnweiher. These measures were ordered by the city of Ludwigshafen. In the framework of these operations, the extensive flat coastal area with a line of artificial islands was constructed on the north side of the lake [77].

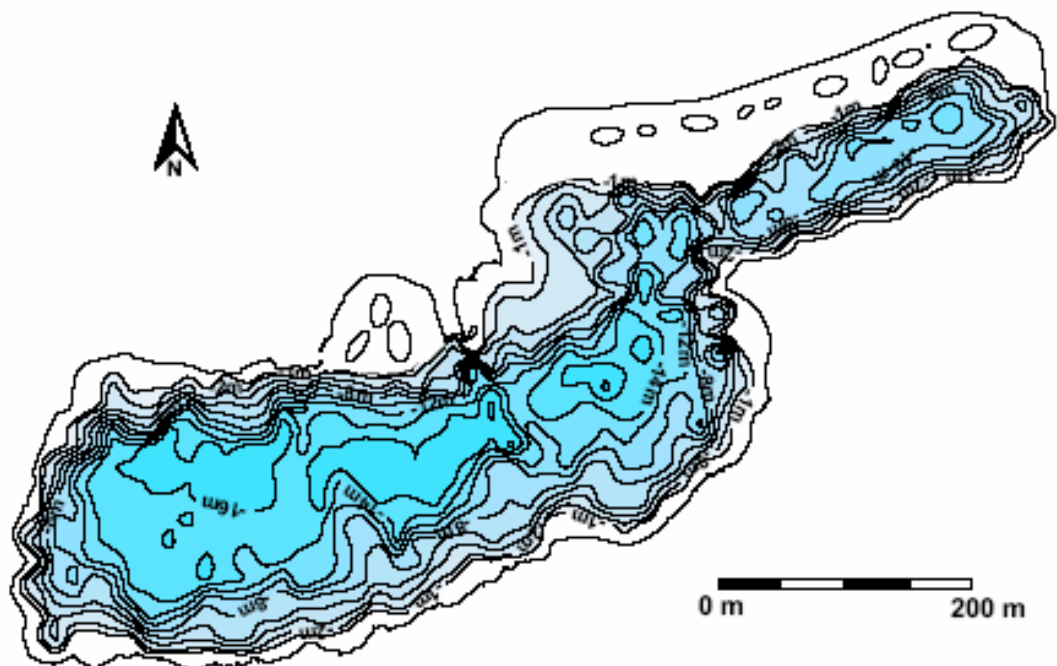


Figure 2.2. Morphological map of Lake Willersinnweiher (Bergner (1997), the map was published by Wollschläger (2003))

2.1.1. Temperature layers and water circulation

Lake Willersinnweiher undergoes seasonal changes. Changes in the temperature profile with depth within a lake system is called thermal stratification. This profile changes from one season to the next and creates a cyclical pattern that is repeated from year to year. Let us begin with spring. In the winter time, the lake water is generally the same temperature from the surface to the bottom. Wind allows circulation and mixing of the lake water. Surface water can be pushed to the lake bottom and bottom water can rise to the surface (Figure 2.3). Schröder (2004) has shown oxygen flux from water column into the sediment in the winter time. According to his research the oxygen penetration into the sediment is 2-2.5 mm.

As air temperatures rise in late spring, heat from the sun begins to warm the lake. The warm water is less dense than the colder water below resulting in a layer of warm water that floats over the cold water. The layer of warm water at the surface of the lake is called the epilimnion. The cold layer below the epilimnion is called the hypolimnion. These two layers are separated by a layer of water which rapidly changes temperature with depth. This is called the metalimnion. In the summer time the top layer temperature is around 18-22°C. Stratification during the summer acts as a deterrent to complete lake mixing. Wind circulates the surface water, but the warm water of the epilimnion is unable to drive through the cold, dense water of the hypolimnion. As a result, the water is only mixed in the epilimnion (Schröder, 2004). During summer the lake bottom water becomes anoxic, and anaerobic bacteria produce hydrogen sulphide gas (H₂S). Schröder (2004) has shown a migration of sulphide in the spring-summer time: at first, the sulphide was observed in bottom water, later it moves up within the hypolimnion, and at the same time the oxygen concentration decreases to zero in this depth.

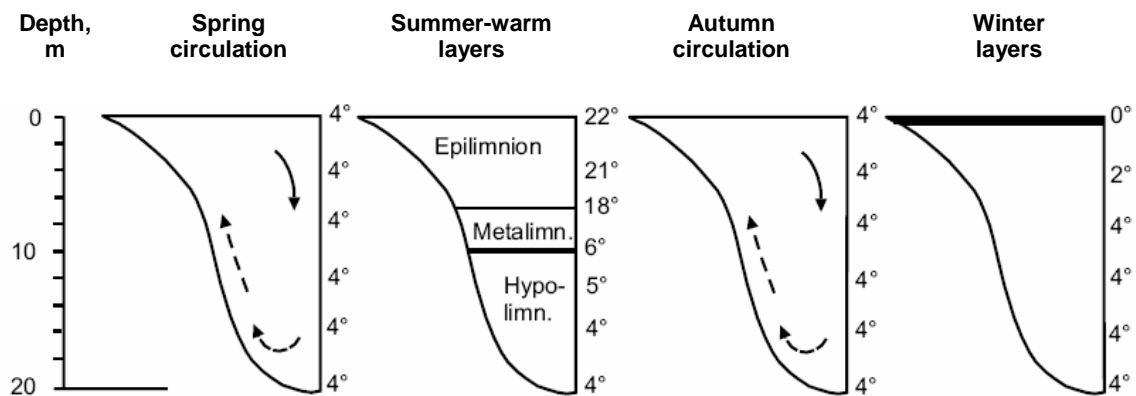


Figure 2.3. Water stratification and circulation varies with temperature (Schwoerbel, 1999)

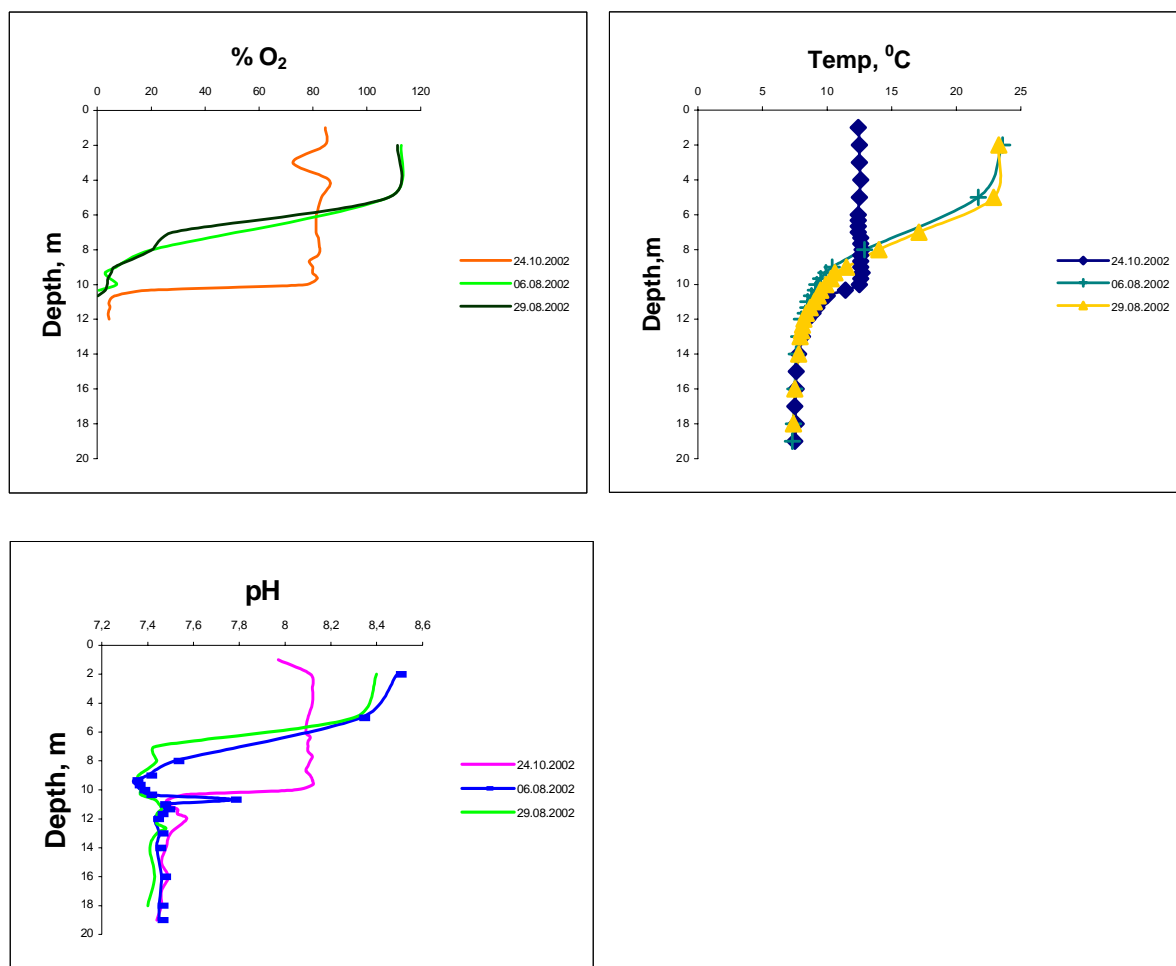


Figure 2.4. Changes of oxygen content, temperature and pH in the water column with depth

Thus the lake has different seasonal conditions in the water column. Figure 2.4 shows the variations of the oxygen content, temperature and pH in the water column in the summer-autumn time. With the alignment of temperature the metalimnion moves down in the water column and during the winter period, oxygen is distributed on the whole water column.

The composition of the water column, elements migration in the water column and ground water transport have already been studied for this lake. Previously, the thermal stratification of the lake has been studied by Laukenmann (2002) and Schröder (2004). Some changes of different elements concentration in the lake water column with depth were summarized by Laukenmann (2002) and Schröder (2004). Schröder (2004) has observed seasonal variations of the redox front by measurements of dissolved iron, manganese, phosphorous, sulphate and sulphide.

2.1.2. Uranium in the water column

Groundwater supplies the main input of uranium. Presumably, the main uranium removal processes in the lake are uranium reduction from U(VI) to U(IV), sorption, and uranium migration between sediment column layers. Figure 2.5 schematically shows the uranium migration in the lake.

The natural uranium concentration in the water column month by month has already been discussed in detail in the dissertation work of Laukenmann (2002). He has already

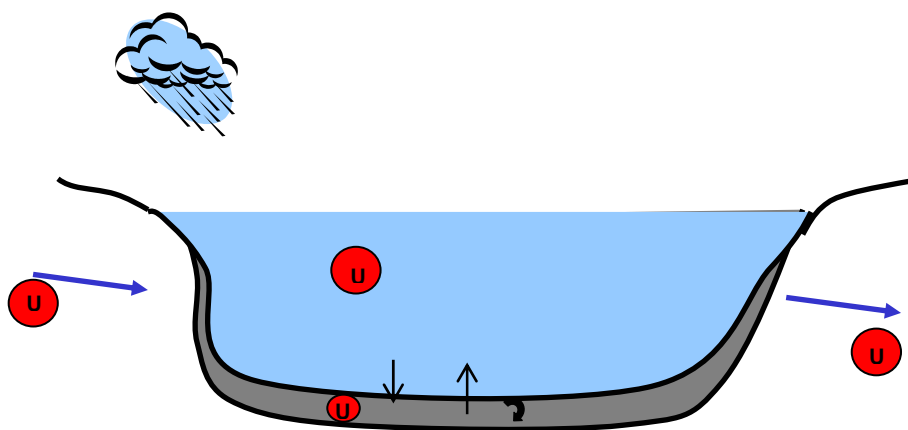


Figure 2.5. Uranium migration in the lake

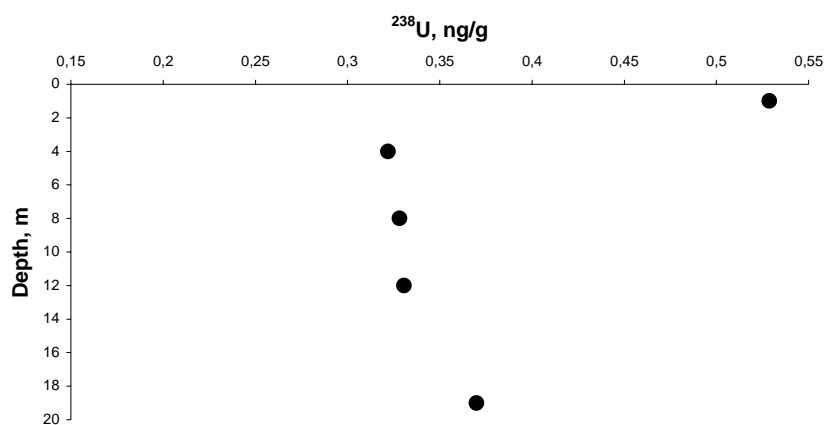


Figure 2.6. Uranium concentration in the water column (10.06.2002)

shown the uranium migration in the water column under different seasonal redox conditions. The average amount of uranium in the water does not vary much in the different seasons. On average the natural uranium concentration in the water column is about $0.30 \mu\text{g/L}$ - $0.35 \mu\text{g/L}$ (Fig. 2.6).

According to literature data uranium is reduced under anoxic conditions. Therefore it is possible to assume that in the summer time uranium reduces to insoluble U(IV) on the interface “sediment-water”; forms particles and penetrates in the sediment as immobile U(IV). An analysis of the pore water was conducted by Laukenmann (2002) (Figure 2.7). These data show that the uranium concentration in the water sharply decreases on the interface “sediment-water”. According to these data it is possible to assume that uranium reduces to insoluble U(IV) on the interface “sediment-water”.

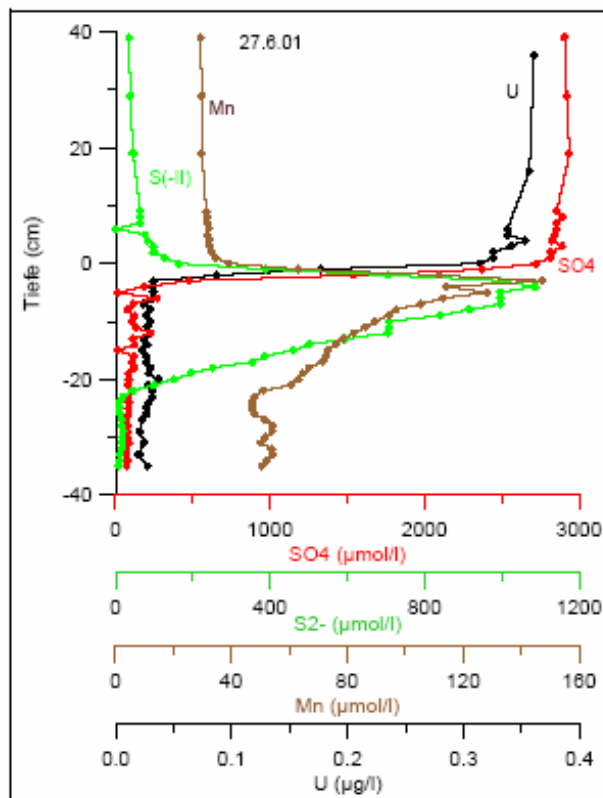


Figure 2.7. Pore water composition (Laukenmann, 2002)

2.1.3. Lake sediment

The water content of the sediment is high; the porosity of the first centimeter is close to 90 % (Fig. 2.8). With increasing depth the sediment consolidates but the porosity does not fall below 74-76 %.

The low density of the sediment is the source of the high degree of interaction between the water column and pore water. This proposes that dissolved uranium can approach relatively easily from a zone of high concentration to one of low concentration in a sediment column.

The mineral composition of the lake sediment is quartz, calcite, albite, clay minerals (chlorite, muscovite, and kaolinite etc); organic matter content is approximately 7%.

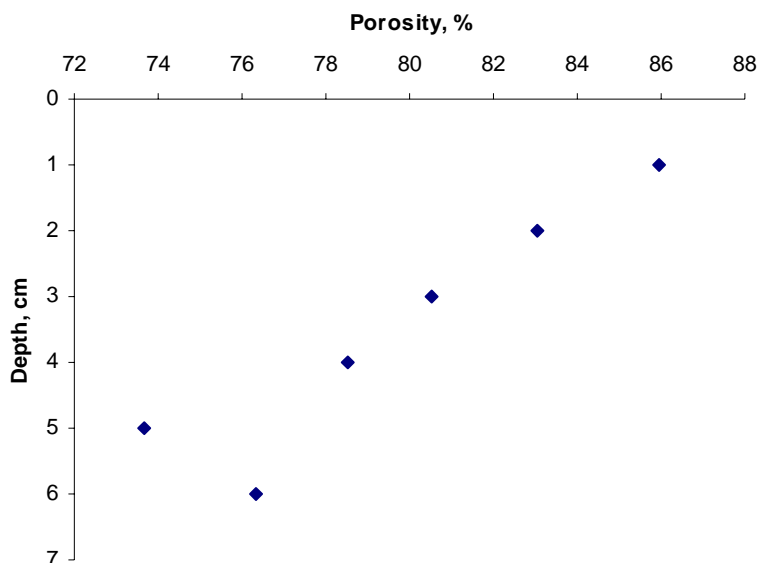


Figure 2.8. Changes of lake sediment porosity with depth

2.1.3.1. Uranium concentration in the sediment column

The prevailing uranium isotope in the lake sediment is ^{238}U , concentration is 1.6-2.8ppm. Another uranium isotope, ^{234}U , is also present in the lake sediment but the concentration of it is low, around $1.3 \cdot 10^{-3}$ ppm. Table 2.1 shows changes of uranium concentration in the lake sediment with depth. The uranium concentration increases which can be explained in two ways: 1) sediments compaction with depth, and 2) uranium is adsorbed by organic matter, organic acids dissolve and diffuse down in the sediment stratum and by this displace uranium in the sediment column. Figure 2.9 shows uranium concentration in ppm scale. The concentration is relatively stable but an increase tend is observe.

Table 2.1. Uranium isotope concentrations

Depth, cm	Uranium concentration (dpm per 1cm of sediment column)	
	^{238}U	^{234}U
1	0.806	0.701
2	0.760	1.214
3	1.140	1.710
4	1.145	1.706
5	2.480	3.700
6	1.892	2.083
7	2.883	3.193
8	3.086	3.349
9	4.202	4.858

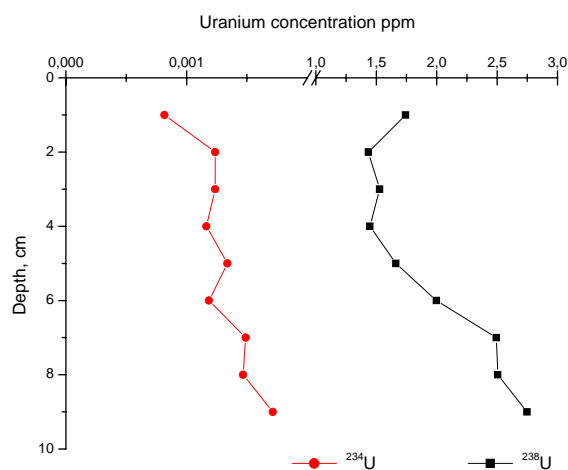


Figure 2.9. Changes of uranium concentration in the sediment column

2.1.3.2. Sediment sample characteristics

Natural sediment samples as well as sediment samples after pre-treatment were used for laboratory experiments (see Chapter 3 Methods). The carbonate content is a major factor controlling uranium sorption.

The characteristics for the two types of sediment are shown in Table 2.2. The methods of sample characteristics determination are described in Chapter 3 (Methods). The calcite dissolution increased twice the Cation Exchange Capacity (CEC) property of the samples.

Table 2.2. Sediment samples characteristics

Sample	Total C (%)	Inorganic C (%)	Organic C (%)	Specific surface area (m ² /g)	CEC (meq/100gm)
Natural sediment	9.66	4.68	4.98	3.87	7.9
Sediment after pre-treatment	6.61	0.00	6.61		13.0

2.2. Calcium carbonate samples

To check another process of uranium immobilization in natural environments as a second object of research coral samples were selected. The samples were provided by D. Scholz.

Corals offer one of the most suitable media for uranium series determination because, after death, coral skeletons mostly act as closed systems until the coral is dissolved or changes to calcite. Uranium series dating of raised coral reef complexes forms the basis for the chronology of Late Quaternary sea-level fluctuation.

However, often isotope ratios for fossils coral do not correspond with the theoretical seawater evolution curve, because the coral appears as an open system, and a part of uranium moves in/out due to different processes (Scholz, 2005).

The studied coral samples were obtained from coral reef terraces from Barbados, the natural uranium concentration of the samples is ~3 ppm. Organic matter content is low (<0.1%). The calcite content is < 5%.

According to literature data [66] the specific surface area of calcite is 0.04 m²/g. The specific surface of an aragonite piece should not differ much from that. For powdered samples

the specific surface area was calculated with the standard graph of surface area versus diameter of particles, resulting is 0.2 m²/g (for the powdered sample with particle size of 125μm).

Chapter 3. Methods

3.1. Sampling

The water sampling procedure is already described by Schmid (2002). Water samples were obtained from every meter of water column in the middle of the lake (depth ca. 19m). While taking water samples, characteristics such as pH (by WTW ph 340), temperature (by WTW LF 330), and O₂ content (by WTW Oxi 232A) were measured.

The sediment–water cores were obtained from the middle of the lake from 19-20 m water-depth. The sampling device consists of a heavy metal pipe with an opening and closing hermetic lid on the top that generates a vacuum when closed. Attached to this at the bottom is a hollow plastic pipe in which the sample is collected. The sampling device was lowered from a boat to the lake-bed (Fig.3.1). The plastic pipe penetrates into the sediment under the weight of the device. The lid at the top of the device is then closed and the resulting vacuum secures the sample in the plastic tube. The sampling device is then winched to the surface with the sediment inside. The size of the sediment cores recovered were around 15 cm long (Fig.3.2).

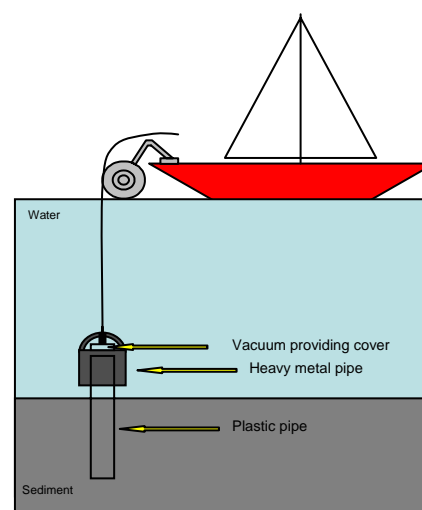


Figure 3.1. Sampling method

3.2. Preparation of samples

To examine the sediment in depth, the sediment core was extracted from the plastic pipe and sampled at 1 cm resolution. The sediment core was then removed from the plastic

pipe with a stick pushed from the bottom. To determine the amount of water in the sediment, the sediment samples were dried in the oven at 105⁰C.

3.3. Investigation of samples



Figure 3.2. Photo of the sediment core in plastic pipe

The mineral composition of the sediment was studied by X-ray diffraction. The measurements were performed with a Siemens D 500 at the Geological-Paleontological Institute of the Heidelberg University. Measurements environment was 40 kV/30mA, using CuKa radiation.

The Cation Exchange Capacity (CEC) was determined by saturating exchange sites with ammonium ions (Research Analytical Laboratory, University of Minnesota).

The specific surface area was calculated from N₂-BET isotherm. Nitrogen adsorption was performed using an automated surface area and pore structure analyser (NOVA 1200, Quantochrome Laboratory) and the samples were degassed at 60⁰C for 17 hours prior to adsorption analysis. A critical point in the use of this procedure is the means by which a multi- or monomolecular

layer is obtained.

The organic matter was determined by the difference between total and inorganic carbon (Research Analytical Laboratory, University of Minnesota).

The elementary analyses were conducted by ICP-MS (Acme Analytical Laboratories Ltd., Canada).

3.4. Uranium determination

The radiochemical yields for natural uranium analyses by alpha spectrometry were determined using ^{232}U as a spike.

The uranium contents for the sorption experiments by alpha spectrometry were determined using ^{238}U as a spike and ^{232}U as a tracer.

The natural uranium concentrations in the water samples were determined by TIMS (Institute of Environmental Physics of the Heidelberg University).

3.4.1. Radiochemical procedure

The first stage in the source preparation process for the alpha spectrometry measurement has to be the complete dissolution of the sample. This was performed by acid digestion using HNO_3 & HCl solutions. Reaction time was 48 hours. Afterwards the sample was filtered and evaporated.

After this pre-treatment, the sample was redissolved in 8 M HCl , and then was purified by anion exchange. For this purpose, the solution was passed through a column with Dowex 1x8 resin in order to eliminate all other elements. After having been washed, the uranium was recovered from the resin with 1 M HCl solution. After the sample was dried and redissolved in $\text{CH}_3\text{COONH}_4$ solution, pH 4.5-5.0, it was then purified by anion exchange. For this purpose, the solution was passed through a column with Dowex 1x8 resin to eliminate Fe element. After having been washed, the uranium was recovered from the resin with 1 M HCl solution.

Finally, the purified solution of uranium was electroplated onto a stainless steel planchet.

Uranium concentration was determined with Alpha-spectrometry.

3.4.2. Alpha-spectrometry

The chemical yields (or extraction efficiencies) of uranium were obtained from the observed ^{232}U count rate in their respective spectra. Table 3.1 shows α -energy for uranium.

Energies of peaks in a sample can be read from the plot of energy (MeV) against peak channel number.

The counting efficiency is given by the expression:

$$E(\%) = \frac{(232)}{0.3 * t * A * V} * 100$$

with

$$\Delta E(\%) = \frac{\Delta 232}{0.3 * t * A * V} * 100$$

t- time of measure (min)

V- spike volume (ml)

0.3 is coefficient of detectors geometry

Spike concentration (dpm/ml)

232- Counts of ²³²U

Uranium concentration:

$$^{238}\text{U}(\text{dpm} / \text{g}) = \frac{238}{0.3 * t * M * (E / 100)}$$

238- Counts of ²³⁸U, M- Mass of assay (g)

Table 3.1. α -energy for uranium

	α - Energy (MeV)	Intensity (%)
²³⁸ U	4.20	77
	4.15	23
	4.04	0.23
²³⁴ U	4.77	72
	4.72	28
	4.60	0.3
²³² U	5.32	68
	5.26	32

3.5. Laboratory experiments

3.5.1. Laboratory simulation of redox conditions

Two seasonal redox situations were simulated in the laboratory in order to understand uranium behaviour in the lake water sediment column.

Two sediment-water columns were obtained from Lake Willersinnweiher in the summer period. In one core the water column had a height of 37 cm, in the second one 22 cm. The sediment column was about 20 cm long. A nitric solution with an artificial isotope of uranium was first neutralized and then added to the water column (initial concentration: 3.51 dpm/ml and 5.91 dpm/ml, respectively). For the first case the uranium trace was added into the anoxic water (the uranium solution was added immediately after sampling and the sediment-water column was kept constantly closed). For the second case the uranium trace was added into the oxygenated water (the sediment-water column was kept open one week before the uranium trace was added). During the experiment the oxygen content was checked several times. Duration of the experiment was 60 days. At the end of the experiment the uranium concentration of the supernatant water was analyzed and then the water was discarded. The sediment was extracted from the core, sampled at 1 cm resolution and centrifuged. The uranium concentrations were determined in the sediment and pore water samples. Experiments were carried out at ambient pressure and room temperature.

3.5.2. Sorption experiments

The uranium adsorption experiments on lake sediments were carried out in the pH range 2-11. The pH of suspension was reached by dint of 1M NaOH and 3.5M HNO₃ solutions in the experiments S1,S1*,S2 and SC, and by dint of buffer solutions in the experiment S3 (pH 2 and 3- citrate buffer, pH 4, 5 and 6- acetate buffer, 8, 9, 10 and 11- borate buffer, at pH 7 distilled water was used). The investigations of uranium uptake by aragonite were carried out at pH range between 6 and 11. All experiments were carried out under oxygenated conditions, ambient pressure and room temperature in 150 ml glass flasks using an artificial uranium isotope (²³²U), total concentration 450dpm (8.14*10⁻¹³M) in 2M HNO₃ matrix.

3.5.2.1. Sample preparation

3.5.2.1.1. Lake sediment

Five sets of experiments (S1, S1*, S2, S3 and SC) with lake sediment were carried out (Table 3.2). To evaluate the effect of mass/volume (M/V) on uranium sorption, experiments were conducted using 0.5, 1.6 and 1.2 g solid in 50 and 100 ml of solution.

The concentration of ^{232}U in dpm scale is high enough for Alpha-measurement, but this concentration is really low in mol ($8.14 \times 10^{-13}\text{M}$). To get uranium atoms in the solution the uranium isotope (^{238}U , 2.78 dpm per assay = $1.66 \times 10^{-8}\text{M}$) was added to the solution before the experiment in set S1*. The concentration of ^{238}U in dpm scale is low and therefore, it does not affect the measurement of uranium with Alpha-spectrometry.

A. Sediment with natural water content (S1, S1*, S2 and S3).

For the sorption experiment the natural wet sediment was used. The sediment core was extracted from the plastic pipe and mixed until homogenous suspension; one sample was obtained to determine the amount of water in the sediment for the subsequent calculation of assay weight.

Table 3.2. Summary of initial experiments condition

Experiment	Initial uranium concentration (^{232}U), M	^{238}U in solution, M	Mass of solid, g	Volume of solution, ml
S1	8.14×10^{-13}	-	0.52+ 0.005	50+0.5
S1*	8.14×10^{-13}	1.66×10^{-8}	0.52+ 0.005	50+0.5
S2	4.07×10^{-13}	-	1.2+ 0.005	100+0.5
S3	8.14×10^{-13}	-	1.6+ 0.005	50+0.5
SC (sediment after "pre-treatment")	8.14×10^{-13}	-	0.7+ 0.005	50+0.5

B. Sediment without calcite (SC).

Carbonate materials were removed from one natural sediment sample by rinsing them in 1M HCl solutions several times. The sample was rinsed free of chloride ion (the sample was washed with distilled water and centrifuged (2000/1h)).

The results of the X-ray diffraction measurement are displayed on Figure 3.3. The absence of calcite peaks for the sediment after pre-treatment suggests that the samples were prepared correctly. The experiments were conducted using 0.7 g solid in 50 ml of solution (Table 3.2).

3.5.2.1.2. Calcium carbonate

A. Uranium sorption by powdered calcium carbonate.

The calcium carbonate sample was powdered in agate ball mills, grain size is < 250 μ m. The experiments were conducted using 0.2 g solid in 50 ml of solution.

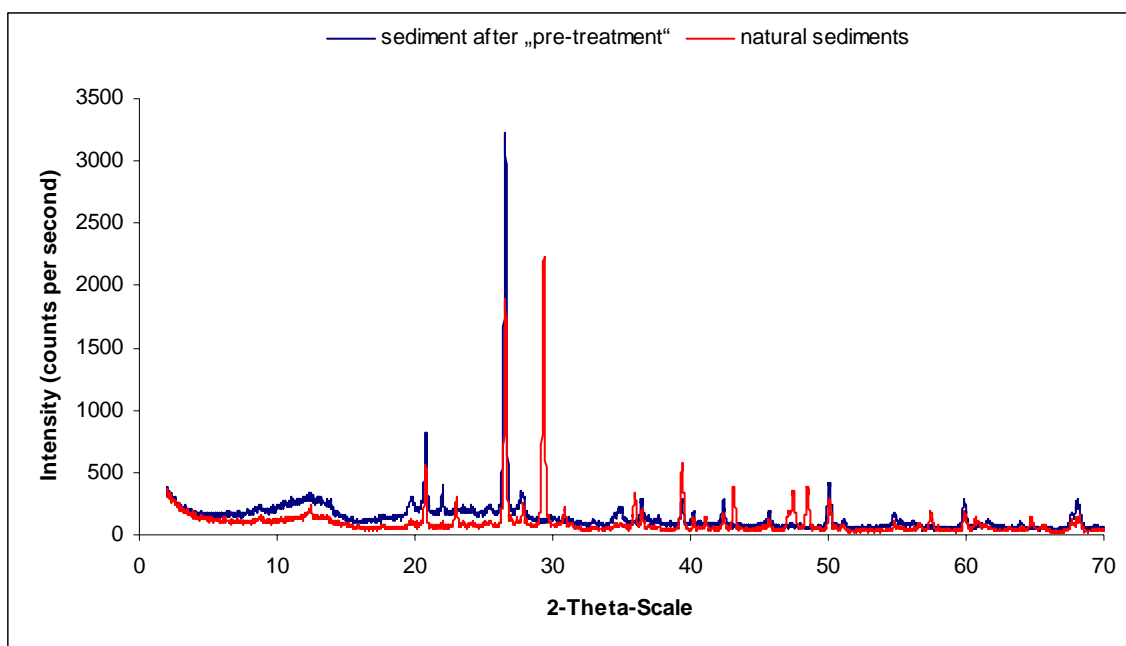


Figure 3.3. X-ray spectra (January 2003)

B. Uranium sorption by aragonite piece.

1g of coral sample, size is 1cm x 1cm x 0.5 cm.

3.5.2.2. Experimental procedure

0.1ml of uranium solution (450 dpm) was added to the distilled water. Then the pH was adjusted with 1M NaOH and 3.5M HNO₃ solutions. Thus the sediment sample was added and the pH of suspension was checked and corrected again.

After a reaction time of 48 hours the pH of suspension was checked again, the solid phase was separated by filtration and then centrifuged. Later the aqueous phase was sampled in order to measure the final uranium concentration; the solid phase was dissolved in HCl and HNO₃ solutions and sampled to measure uranium concentration.

3.5.3. Desorption

The sediment sample (3 g) was kept in a uranium solution for 60 days. After the reaction time the supernatant water was extracted and sampled to determine uranium concentration. The uranium enriched sediment was placed into a 500 ml glass flask and covered with distilled water (300 ml). The suspension was kept open to atmosphere CO₂(g) for 18 days. During the experiment, suspension was constantly agitated and water was periodically added to keep the volume of suspension around 300 ml. After reaction time the uranium concentration was determined in supernatant water, pore water and in the sediment. The desorption percentage concentration was calculated assuming a total uranium adsorption concentration in the sediment substrate equal to a value of 100%.

A. Desorption experiments at pH range between 2-11.

After the reaction time, the first solution was extracted and sampled in order to determine uranium concentration; the sediment sample was covered with another solution with the same pH. Reaction time of desorption was 24 hours. After this reaction time the uranium concentration in water and sediment samples was determined.

3.5.3. Column experiment

For these experiments a plastic column (Poly-Prep column, 9 cm high, 0.5 cm diameter, Figure 3.4) with filter was used. The aragonite fragment was crashed with a hammer in order to get relatively large particles (grain size was about 250 μ m and larger). This grain size can provide good water filtration. To evaluate the effect of filtration time experiments were conducted using 0.2, 0.44, or 1.5 g of solid. The sets of experiments are displayed in Table 3.3.



Figure 4.3. Poly-Prep column

Method of experiment:

First the column was filled with powdered sample, after that the solutions were filtered through the column:

1. 30 ml of distilled water was filtered through the column to move off colloids and small particles, which can pass through the filter.
2. 25 ml of uranium solution (450 dpm, ^{232}U in 2M HNO_3 matrix neutralized with 2M NaOH and dissolved in distilled water, pH of solution was 7) was filtered through the sample. The aliquot of filtered solution was sampled to determine uranium concentration.
3. 25 ml of distilled water was filtered through the sample. The aliquot of filtrate was sampled to determine uranium concentration.

Table 3.3. Sets of column experiments

Experiment	Mass of solid, g	Time of filtration (25 ml), min
K1	0.2	6
K2	0.44	12
K3	1.5	20

4. 50 ml of distilled water was filtered through the sample. The aliquot of filtrate was sampled to determine uranium concentration.
5. 150 ml of distilled water was filtered through the sample. The aliquot of filtrate was sampled to determine uranium concentration.

Chapter 4. Results & Discussion

4.1. Redox simulation

As it has already been described above (see Chapter 2) Lake Willersinnweiher has different redox conditions in the water column during the summer and winter time. In order to understand the uranium migration in the lake the two types of seasonally redox conditions were simulated in the laboratory using an artificial uranium isotope, ^{232}U . The initial uranium concentration in the water column was 3.6 dpm/ml (see Chapter 3 Methods, 3.5.1. Laboratory simulation of redox conditions). In order to simulate two different situations, the uranium solution (1800 dpm) was added to the anoxic water column in the first case, and to the oxic water column in the second case (see Chapter 3).

In both cases (under oxic and anoxic conditions) 80 % of uranium penetrated into the sediments. After two months the uranium concentration was ~ 0.3 dpm/ml in the water column (Table 4.1). The uranium concentrations (^{232}U) in sediment after reaction time are shown in the Figures 4.1 and 4.2. Table 4.1 shows uranium balance in the experiment.

Under anoxic conditions, “Summer” type, (Figure 4.1) 80 % of uranium is fixed in the first centimetre of the sediments, probably in the first few millimetres (it is difficult to measure less than 1 cm of sediment due to high porosity).

In contrast to the first experiment, uranium in the oxygenated water column (“Winter” type) penetrated deeper into the sediments (Figure 4.2). Uranium penetration is ca. 4 cm. These results show that uranium diffused with pore water into the sediment and was absorbed.

Results of this study show that uranium in the water column accumulates in the sediments under oxic and anoxic conditions (in the “summer” and “winter” type). Uranium does not diffuse deeper into the sediment column under anoxic conditions, thus marking a layer of sedimentation in this period (Fig.4.1). One possibility to explain it may be uranium reduction by anaerobic bacteria on the interface “sediment-water”. In this case uranium forms particles and co-precipitates with the creation of the sediment layer. In this study no measurement of uranium valence was conducted therefore I can not assert that uranium is reduced to U(IV).

Under oxic condition (in the "Winter" type) dissolved uranium diffuses deeper into the sediment column with pore water (Fig.4.2).

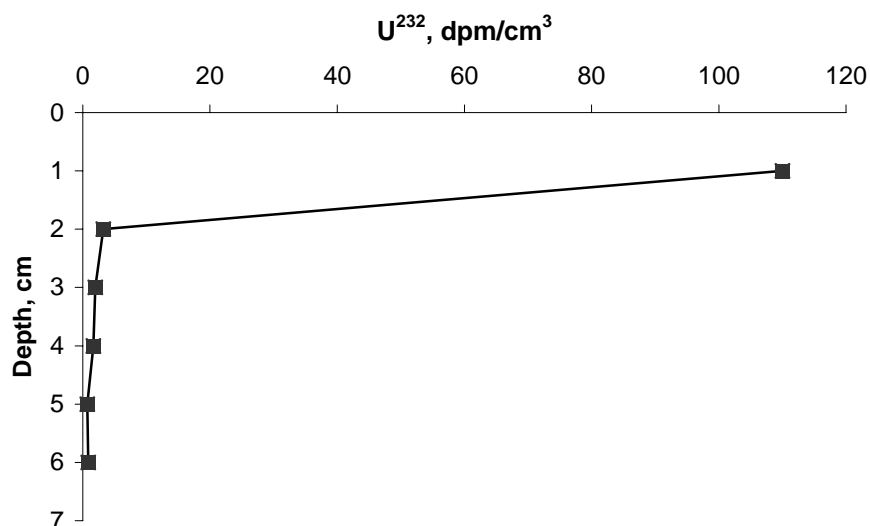


Figure 4.1. Uranium concentration in the sediment after experiment under anoxic conditions, "summer" type

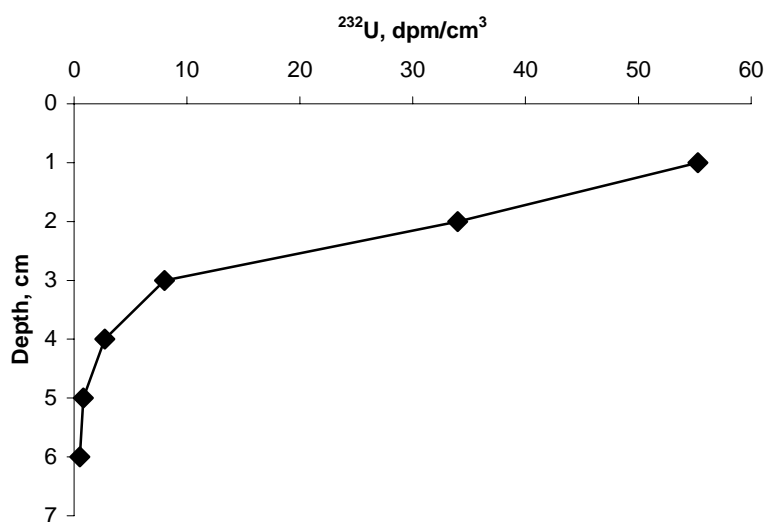


Figure 4.2. Uranium concentration in the sediment after experiment under oxic conditions, "winter" type

Table 4.1. Uranium balance in the experiment

		Uranium concentration, dpm per cm of column	
		1 st case (under anoxic conditions)	2 nd case (under oxic conditions)
Sediment	1 st cm	1541.50	851.06
	2 nd cm	44.83	501.07
	3 rd cm	27.54	121.58
	4 th cm	23.03	45.59
	5 th cm	9.38	11.37
	6 th cm	11.79	7.03
Pore water	1 st cm	6.47	10.74
	2 nd cm	1.33	4.48
	3 rd cm	0.58	3.26
	4 th cm	0	2.10
	5 th cm	0	1.08
Uranium concentration			
In complete water column		143.59 dpm (0.28 dpm/ml X 512ml)	121.83 dpm (0.4 dpm/ml X 304ml)
Total (in the sediment, pore water and water column)		1810.05 dpm	1681.65 dpm
²³² U before experiment		1800 dpm	1800 dpm
Experiment error		-10.05 dpm	118.35 dpm

4.2. Lake sediment

4.2.1. Uranium (VI) adsorption at pH range between 2-11

Experiment sets: S1, S1*, S2, S3 and SC

The uranium accumulation in the sediments could be provided for in different ways, for example:

- Uranium sorption as uranyl ion (UO_2^{2+}) onto a mineral surface.
- Uranium sorption as uranium carbonate complex ($\text{UO}_2(\text{CO}_3)_2^{2-}$ and $\text{UO}_2(\text{CO}_3)_3^{4-}$) onto an iron or aluminium oxides surface.

-Uranium incorporation as uranium carbonate complexes ($\text{UO}_2(\text{CO}_3)_2^{2-}$ and $\text{UO}_2(\text{CO}_3)_3^{4-}$) into calcium carbonate.

The mineralogical study (see Chapter 2, Samples) showed the high calcite content in the natural sediment samples and previously, J. Schmid (2002) showed calcite formation in Lake Willersinnweiher.

In order to estimate calcite influence on the uranium sorption process, laboratory experiments were carried out with natural sediment and with sediment without calcite (calcite was removed from the natural sediment; see Chapter 3, Methods, 3.5.2.1.1.B. *Sample preparation*). The study of the elementary composition showed the same uranium concentration for natural sediments and for sediments without calcite (Table 4.2). Table 4.2 displays the results of ICP-MS Analysis (see Chapter 3, Methods) on sediment samples before sorption experiments. These results suggest that calcite in the natural sediment does not contain uranium.

The results of the uranium sorption experiments are displayed in Figure 4.3. The sets characteristics are described in Chapter 3 Methods, 3.5.2. *Sorption experiments*. The data of uranium sorption by sediments is shown in this graph as a function of pH. These results demonstrate the strong pH dependence of uranium sorption. The maximum amount of sorbed U(VI) on this sediment was reached at pH 7, and decreased sharply towards more acidic or more alkaline conditions. Like most cations, adsorption of uranium increases with increasing pH, but at higher pH a decrease of sorption takes place. This pH dependence of uranium sorption has also been observed with different mineral sorbents, such as quartz and other silicates minerals and aluminium and iron oxides [20, 48, 52, 68]. For example, Arnold et al.

Table 4.2. Elementary composition (only selected components)

Sample	Element	Fe %	Ca %	U ppm
Natural sediment (S1,S2, S3)		2.1	16.07	1.8
Sediment after "pre-treatment" (SC)		2.02	0.26	1.8

(1998) report the sorption edges of uranium onto different solids. These authors found that maximum sorption was observed in the pH range from 5.5 to 8.5 for phyllite, and from 6 to 7 for the minerals composing phyllite: chlorite, muscovite, quartz and albite. A sharp decrease of uranium sorption at lower pH range (pH from 3 to 6) indicates that ion-exchange interaction between the uranyl species and the exchange cations in sediment were suppressed in the NaNO₃ matrix [52].

Figure 4.3 shows the different U(VI) adsorption in the pH range between 9 and 11: the natural sediment (S1, S2, and S3; initial experiments condition is shown in Table 4.3. The main difference between experiments sets is Mass/Volume ratio) sorbs less uranium compared to sediment with pre-treatment (SC).

Table 4.3. Summary of initial experiments condition

Experiment	Initial uranium concentration (²³² U), M	²³⁸ U in solution, M	Mass of solid, g	Volume of solution, ml
S1	8.14*10 ⁻¹³	-	0.52+ 0.005	50+0.5
S1*	8.14*10 ⁻¹³	1.66*10 ⁻⁸	0.52+ 0.005	50+0.5
S2	4.07*10 ⁻¹³	-	1.2+ 0.005	100+0.5
S3	8.14*10 ⁻¹³	-	1.6+ 0.005	50+0.5
SC (sediment after “pre-treatment”)	8.14*10 ⁻¹³	-	0.7+ 0.005	50+0.5

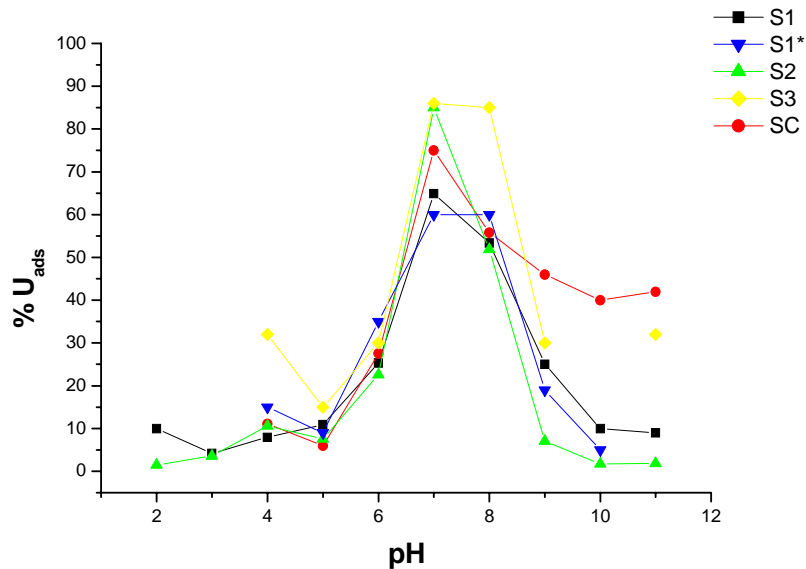


Figure 4.3. Sorption of U(VI) by the natural lake sediment and by the sediment after “pre-treatment”

Representing the U(VI) sorption data in terms of a distribution coefficient (K_d) as a function of pH normalizes the effect of changes in M/V and accounts for the effect of changes in U(VI) solution concentration (Figure 4.4).

The K_d is defined as:

$$K_d (\text{ml/g}) = \frac{\text{amount of U(VI) sorbed/gram of solid}}{\text{amount of U (VI) in solution after experiment/ml of solution}}$$

(R.T.Pabalan et al., 1997) [52].

This representation of experimental data is very useful, because when sorption is near to saturation, the variations are better detected, thus simplifying the fitting procedures [52].

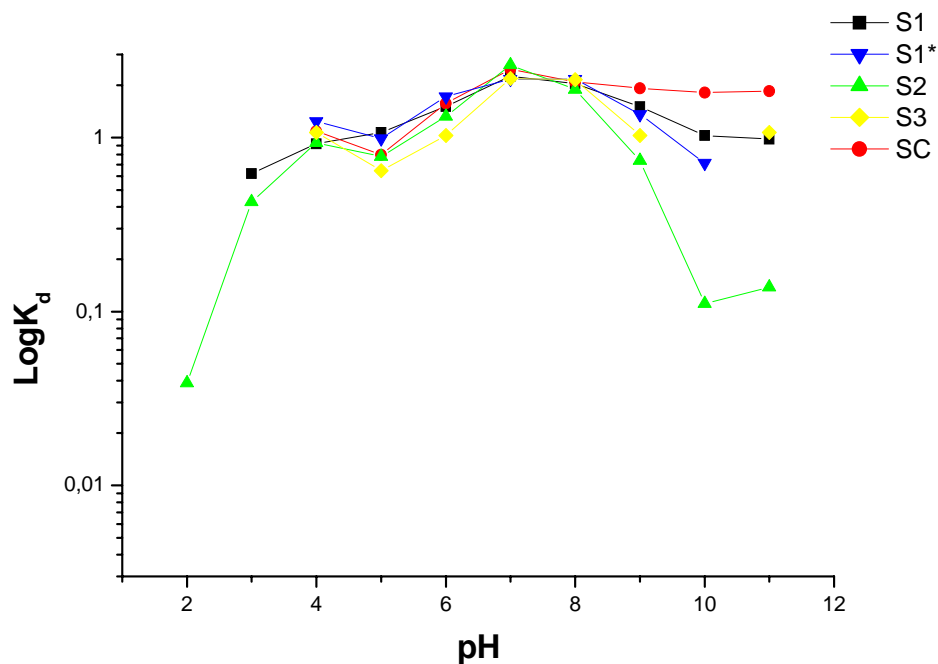


Figure 4.4. Sorption of U(VI) by the natural lake sediment and by the sediment after “pre-treatment” in terms of LogK_d versus pH

Figure 4.4 shows that U(VI) adsorption does not vary much with changes in M/V in the pH range between 4 and 8. In this pH range the calcite content in solid phase is unimportant: the U(VI) adsorption by natural sediments and sediment with pre-treatment is the same.

These data show that uranium sorption increases with increasing uranium concentration in solution at higher pH. At high pH range the uranium adsorption on natural sediment (S1, S1*, S2 and S3) depends on the initial uranium solution concentration. The uranium concentration for the sets S1, S1* and S3 is 450 dpm in 50 ml, that means $8.14 \cdot 10^{-13}$ M. The uranium concentration for the set S2 is 450 dpm in 100 ml, which means that the molarity is twice as low ($4.07 \cdot 10^{-13}$). The adsorption decreases sharper in the experiment with lower uranium concentration in the solution (S2) compared to experiments S1 and S3.

This study shows that in the pH range between 4 and 8 the process of U(VI) adsorption is provided by the same mechanism, both in the sediment with calcite as well as in the sediment without calcite. With increasing pH the process of U(VI) adsorption by natural

sediment decreases due to the formation of aqueous anionic U(VI)-carbonate complexes. The sorption ability of these U(VI)-carbonate complexes depends on the uranium concentration in the initial solution and the M/V ratio. As the sorbate to sorbent ratio increases, the adsorption amount shifts to higher pH values. The experiments S1 and S3 show an increase of a U(VI) sorption amount in the pH range between 9 and 11.

In the pH range 4-8 there is no fundamental difference between the adsorption mechanisms in neither cases.

The molar uranium concentration, which was used for experiments, is relatively low (450 dpm in 50 ml = $8.14 \cdot 10^{-13}$ M). To increase molarity the uranium spike ^{238}U (2.78 dpm in 50 ml = $1.66 \cdot 10^{-8}$ M) was added into the solution in set S1* (see Chapter 3, Methods). Thus the difference between the initial condition in sets S1 and S1* is only the uranium concentration in the initial solution. The changes between uranium sorption by sediment in set S1* and in set S1 can be considered as “not significant”. That means that despite the increase the uranium concentration in the solution is not sufficiently high to affect changes in uranium sorption.

4.2.2 Desorption

A sediment sample was enriched with uranium (^{232}U) for 60 days (see Chapter 3, Methods, 3.5.3 Desorption). The total uranium concentration after reaction time was 412 dpm. After reaction time the supernatant solution was removed and the sediment sample was covered with distilled water, the pH of suspension was between 6 and 7. After desorption time the uranium concentration in water was 0.5 dpm/ml, in pore water 1.4 dpm and in the sediment sample 272 dpm.

Desorption of adsorbed uranium after 18 days is 34%.

4.2.2.1. Desorption at pH range 2 –11

Figure 4.5 shows the uranium desorption after 24 hours in pH range between 2 and 11. The maximal amount (32-42 %) of desorption is at pH range between 2 and 4. At nearly neutral and high pH the desorption is minimum.

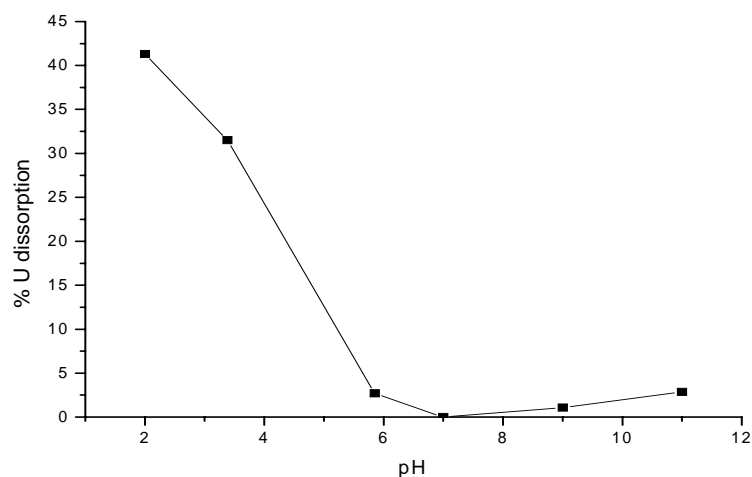


Figure 4.5. Desorption of uranium after 24 hours at pH range between 2 and 11

4.2.3. Adsorption at pH 7

The maximal amount of uranium adsorption is at pH 7. Figure 4.6 shows U(VI) sorption on lake sediment at pH 7 versus uranium concentration in the initial solution. This graph illustrates that U(VI) adsorption after 24 hours reaches 86-97 % in experiments with different uranium concentration (Fig. 4.6). The changes in adsorption amount are not significant, perhaps, due to low uranium concentration. The ^{232}U molar concentration in range between 10 and 80 dpm (10 dpm in 50 ml = $1.81 \cdot 10^{-14}\text{M}$) is really low. Therefore uranium sorption is at the maximum level and adsorption isotherm provides no information. A tendency of adsorption decreasing with decreasing uranium concentration in this concentration range was not observed.

In order to compare the U(VI) adsorption on the sediment at pH 7 with other minerals, other sorption experiments with clay “standard” were carried out. Figure 4.7 illustrates the sorption data at pH 7 for sediment samples with different pre-treatment, kaolinite, muscovite, montmorillonite and biotite.

The U(VI) sorption amount is practically the same. The sorption decrease is observed in the dry sediment sample. This can be a result of changes in density and structure of the sediment due to drying.

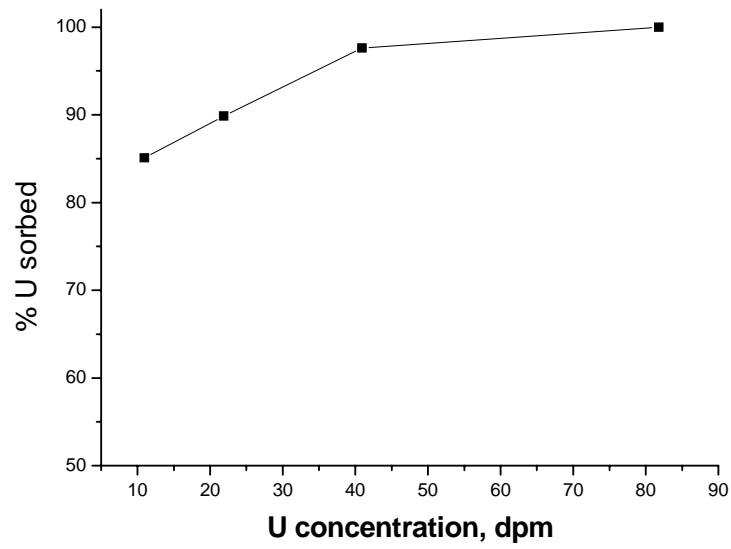


Figure 4.6. Uranium adsorption by the lake sediment at pH 7

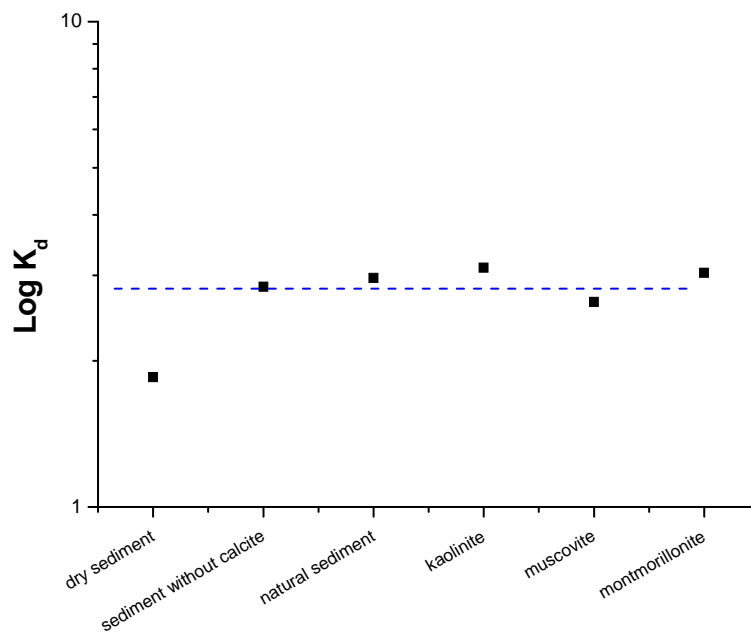


Figure 4.7. Uranium sorption onto different mineral surface at pH 7

4.2.4. Summary

Results from the study suggest that uranium from the water column accumulates in the sediments as well under reduced as under oxygenated conditions. In reduced water, uranium reduces from U(VI) to U(IV), forms particles and co-precipitates. Uranium location in the first centimetre of sediments in column experiment indicates this. In the oxygenated water dissolved uranium penetrates with pore water in the sediments and sorbs there.

Sorption experimental data indicate that U(VI) strongly sorbs onto poly-component materials such as lake sediments. The U sorption is strongly dependent on pH, and the maximum amount of sorption is in the neutral pH range. The calcite content at neutral pH is unimportant, but at high pH it decreases the sorption process. The natural pH condition on the interface “sediment-water” is in the pH range between 7 and 8. The sorption experiments show that in this pH range uranium adsorption on sediment is at its maximum level. This confirms the creation of authigenic uranium in sediment due to adsorption from the water column.

4.3. Uranium uptake by calcium carbonate

Reeder et al. 2000 showed already that uranium uptake by calcium carbonate occurs due to uranium incorporation in solids (see Chapter 1).

In the following chapters this study shows some factors, which influence uranium incorporation in calcium carbonate.

4.3.1. pH influence on U(VI) uptake

With the same method of uranium sorption (See chapter 3, Methods) the laboratory sorption experiments with powdered coral were carried out at pH range between 6 and 11. Figure 4.7 shows that uranium uptake by powdered coral is strongly dependent on pH. The maximum amount of U(VI) uptake (98%) is at pH 7.

The uranium uptake decreases with increasing pH. With a higher pH range the U(VI) uptake amount decreases to 20 %.

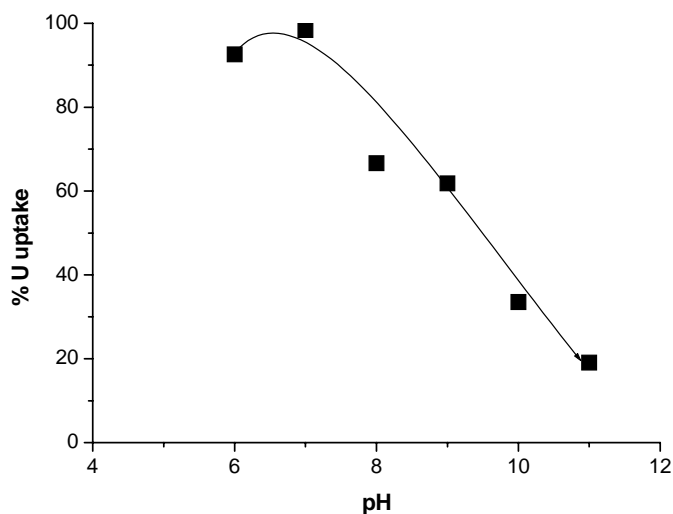


Figure 4.8. Uranium uptake by powdered coral at pH range between 6 and 11

4.3.2. Uranium uptake at pH 7

Figure 4.9 shows the uranium uptake at pH 7 for a powdered sample and a piece of aragonite after 24 hours. The maximum amount of U(VI) uptake takes place at pH 7 using powdered aragonite and reaches 100 %, whereas U(VI) uptake, with a mineral piece reaches 12 %. This suggests uranium uptake dependence on specific surface areas (see data of specific surface areas in Chapter 2). The maximum concentration of dissolved calcium carbonate is 0.006 g/L. The structural connections are destroyed in the powdered sample. Therefore the sample dissolves relatively fast. The coral piece needs more time for dissolution in comparison with the powdered samples.

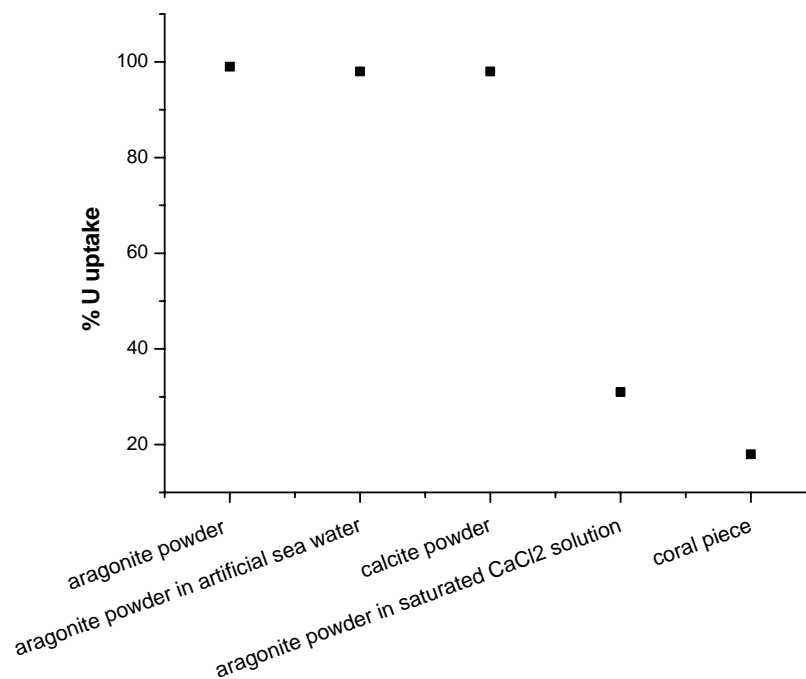


Figure 4.9. Uranium (VI) uptake at pH 7

Furthermore in Figure 4.9 the uranium uptake for aragonite and calcite samples is displayed. This result shows no difference in U(VI) uptake by powdered minerals, but it decreases in saturated CaCl₂ solution.

4.3.2.1. Kinetic experiment

In order to examine U(VI) uptake dynamics by mineral piece, kinetic experiments were conducted for the coral piece at constant pH (pH 7) and ionic strength. The results are plotted as function of time.

Figure 4.10 shows that uranium uptake by coral piece reaches 80 % after 60 days.

That means that uranium uptake is dependent on carbonate mineral possibility to dissolve in a solution. Because uranium co-precipitation with calcium carbonate realize by the following: carbonate dissolves in a solution, carbonate ions form uranium carbonate complexes, and “new uranium-carbonate” precipitates

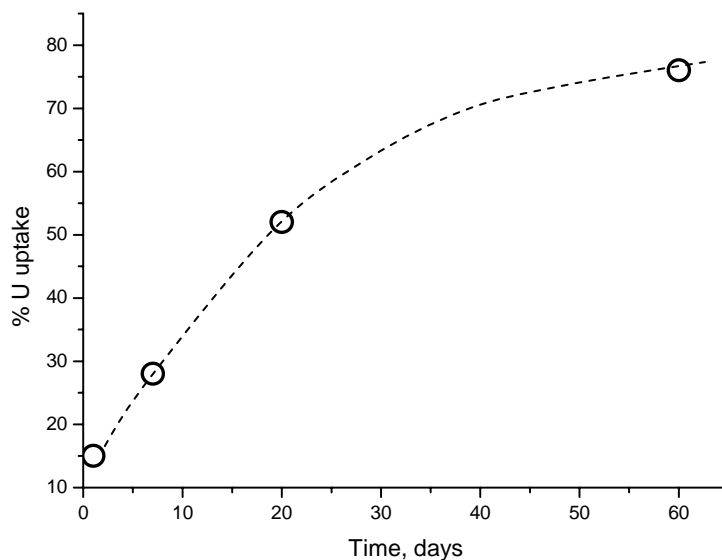


Figure 4.10. Kinetic of uranium uptake by coral piece

4.3.2.2. Influence of solution compound

The influence of solution composition on U(VI) uptake by powdered aragonite is shown in this experiment.

The uranium uptake and XCl (any chloride) concentration for coral samples given in Figure 4.11 indicate that at low concentrations (0.001 M) the uranium uptake amount is 100 %. Decreasing uranium uptake corresponds with increasing XCl concentration. Also the decrease of U(VI) uptake amount is dependent on supernatant solution compounds. The decrease of uptake amount is sharp in MgCl₂ and NaCl solutions.

The concentration of XCl in natural seawater is:

NaCl	~ 0.4 M
KCl	~ 0.009 M
CaCl ₂	~ 0.01 M
MgCl ₂	~ 0.05 M

According to the results, the concentration of K, Ca, and Mg chlorites are insufficiently high and cannot therefore influence the uranium uptake (Fig. 4.11). However, sodium chlorite concentration in seawater is high enough. The sorption results on Figure 4.11

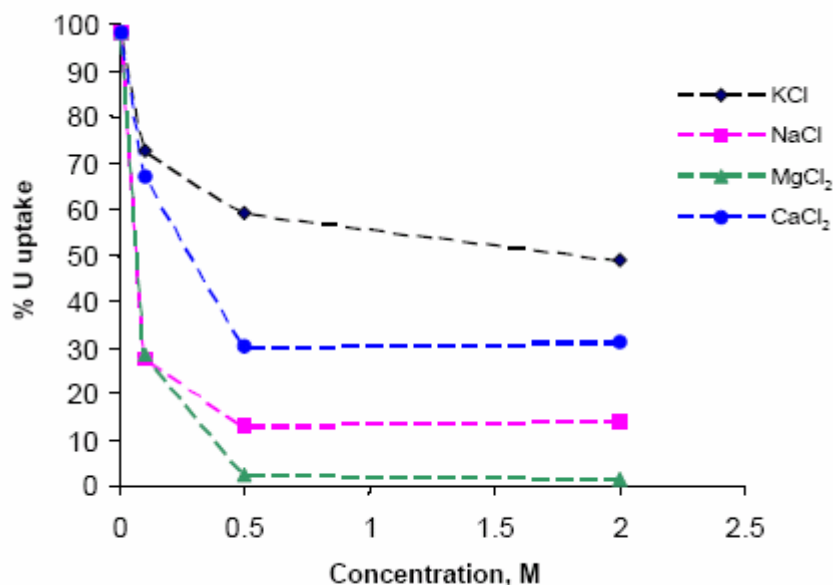


Figure 4.11. Uranium uptake by powdered aragonite at pH 7 in different solutions

show that uranium uptake strongly decreases in sodium chlorite solution in a concentration range between 0.1M and 0.5M.

4.3.2.3. Transport experiment

To estimate uranium uptake by powdered mineral the “column experiment” was conducted (see Chapter 3, Methods, 3.5.3. Column experiment). The uranium solution (450dpm) was filtered through the plastic column with powdered aragonite. After this, distilled water was filtered. The results are presented in Table 4.4.

During solution filtration, uranium immobilizes due to interaction with carbonate particles. The subsequent repeated elution with distilled water does not take out uranium from the column, although distilled water was filtered through the samples several times after uranium enrichment. This confirms that uranium remains stable in the aragonite sample and this uranium immobilization is stronger than uranium adsorption on the particle surface. A 100% uptake of uranium after filtration time of 20 min suggests a relatively fast uranium incorporation.

Table 4.4. Results of column experiment

Experiment	Mass of solid, g	Time of filtration (25 ml), min	% Uranium in water			
			1 st 25 ml (uranium solution)	2 nd 25 ml	50ml	150 ml
K1	0.2	6	42	9	0	0
K2	0.44	12	54	5	0	0
K3	1.5	20	0	0	0	0

4.3.3. Summary

Uranium uptake by calcium carbonate is strongly pH dependent and the maximum amount is reached at pH 7. The time of U(VI) uptake is dependent on the specific surface area. In the system “distilled water-powdered aragonite sample” uptake is fast due to short time of calcium carbonate dissolution. Thus uranium uptake depends on the time of calcium carbonate dissolution.

Also due to slow dissolution of the coral piece, after 24 hours the U(VI) uptake reaches just 10 % but after 60 days uptake reaches 78%.

Uranium uptake is dependent on the solution composition also because of the decrease of calcium carbonate dissolution.

Chapter 5. Model of the uranium adsorption process onto the sediment surface

One of the aims of the work is to fit the experimental data with the simplest model capable to reproduce it and to simulate the influence of changing initial conditions on uranium sorption behaviour.

The modelling of the sorption experiments was carried out with the classical diffuse double layer model (DLM), Dzombak and Morel (1990) (see Chapter 1, 1.2. *A model of the Uranium adsorption*). The model was used by Barnett et al. (2002) for the adsorption of U(VI) to heterogeneous subsurface media [6]. The degree of adsorption of aqueous ions is explicitly corrected for the pH-dependent charge of the ferrihydrite surface. The model was used to predict the pH-dependent adsorption of U(VI) on Oak Ridge soil. The results of this study indicate that the model was able to predict the major features of pH-dependent adsorption to all three media: the sharp increase in adsorption from pH 3 to pH 5 (i.e., the “first” pH adsorption edge), the plateau in adsorption from pH 5 to pH 8, and the dramatic decrease in adsorption from pH 8 to pH 9 (i.e., the “second” pH adsorption edge).

Equilibrium constants for aqueous U(VI) hydroxo and carbonate complexes were taken from Barnett et al. 2002. These species and their constants are summarised in Table 5.1.

The model equations were solved using Visual MINTEQ 2.31. The program is available to free download on the website:

<http://www.lwr.kth.se/English/OurSoftware/vminteq/> .

5.1. Modelling

The speciation as a function of the pH for uranium concentration of $8 \cdot 10^{-14}$ mol/L was calculated, supposing a zero partial pressure of CO₂. The calculated aqueous speciation with the data of Table 5.1 at ionic strength 0.1 and absence carbonate is shown in Figure 5.1. The dominant species at pH < 5 are UO₂²⁺ and UO₂OH⁺. At pH between 6.5 and 8, UO₂(OH)₂ becomes the major dissolved species, whereas at higher pH the negatively charged UO₂(OH)₃⁻ predominates.

Chapter 5. Model of the uranium adsorption process onto the sediment surface

The calculated aqueous speciation in carbonate system ($[\text{CO}_3^{2-}] = 6 \cdot 10^{-5}$) at ionic strength 0.1M is shown in Figure 5.2. At pH <7.5 uranium carbonate complexes become the major dissolved species $\text{UO}_2(\text{CO}_3)_3^{4-}$ and $\text{UO}_2(\text{CO}_3)_2^{2-}$.

Since the U(VI) aqueous speciation is complex, different complexes can be postulated and a unique modelling approach does not exist.

The application of surface complexation approaches to complex solids, such as silicates implies an additional difficulty because of the presence of different functional groups on the surface of the solid: $>\text{SiOH}$ and $>\text{FeOH}$ in the case of lake sediment. For sake of simplicity, the diffuse double layer model was therefore applied considering only one unique type of sorption sites: SOH [21, 48, 49]. In fact, this simplification has been followed by several authors (Sverjensky and Sahai, 1996; Wanner et al., 1992; El Aamrani et al., 2002, Missana et al., 2003 and other). U(VI) is a hard type cation with strong affinity for oxo and hydroxo groups. This is why uranium is sorbed onto mineral surfaces via co-ordination to the surface terminal $-\text{OH}$ function groups [21]. A large amount of work has been devoted to the study of the sorption of uranium onto many different oxy-hydroxides (His and Langmuir, 1985; Missana et al., 2003; Barnett et al., 2002). Oxides and hydroxides present, in general, a large sorption capacity than silicates [21]. So far as the maximal uranium sorption is onto the surface of iron-oxides (See Chapter 1) and the sediment from Lake Willersinnweiher contains iron, the constants of iron-uranium interaction reactions were used as a basis.

The specific surface area of the natural sediment sample was determined (see Chapter 3, *Methods*) the value was $3.87 \text{ m}^2/\text{g}$. The specific surface area of sediment after pre-treatment

Table 5.1. Reaction included in Model (T=25 °C), from Barnett et al. (2000)

U(VI) Aqueous Complexation Reactions	Log K
$\text{UO}_2^{2+} + \text{H}_2\text{O} \leftrightarrow \text{UO}_2\text{OH}^+ + \text{H}^+$	-5.41
$\text{UO}_2^{2+} + 2\text{H}_2\text{O} \leftrightarrow \text{UO}_2(\text{OH})_2^0 + 2\text{H}^+$	-12.23
$\text{UO}_2^{2+} + 3\text{H}_2\text{O} \leftrightarrow \text{UO}_2(\text{OH})_3^- + 3\text{H}^+$	-20.00
$\text{UO}_2^{2+} + 4\text{H}_2\text{O} \leftrightarrow \text{UO}_2(\text{OH})_4^{2-} + 4\text{H}^+$	-32.57
$3\text{UO}_2^{2+} + 5\text{H}_2\text{O} \leftrightarrow (\text{UO}_2)_3(\text{OH})_5^+ + 5\text{H}^+$	-16.22
$4\text{UO}_2^{2+} + 7\text{H}_2\text{O} \leftrightarrow (\text{UO}_2)_4(\text{OH})_7^+ + 7\text{H}^+$	-22.62
$2\text{UO}_2^{2+} + 2\text{H}_2\text{O} \leftrightarrow (\text{UO}_2)_2(\text{OH})_2^{2+} + 2\text{H}^+$	-5.79
$3\text{UO}_2^{2+} + 7\text{H}_2\text{O} \leftrightarrow (\text{UO}_2)_3(\text{OH})_7^- + 7\text{H}^+$	-31.29
$2\text{UO}_2^{2+} + \text{H}_2\text{O} \leftrightarrow (\text{UO}_2)_2\text{OH}^{3+} + \text{H}^+$	-2.44
$3\text{UO}_2^{2+} + 4\text{H}_2\text{O} \leftrightarrow (\text{UO}_2)_3(\text{OH})_4^{2+} + 4\text{H}^+$	-12.25
$\text{UO}_2^{2+} + \text{H}_2\text{CO}_3 \leftrightarrow \text{UO}_2\text{CO}_3^0 + 2\text{H}^+$	-6.80
$\text{UO}_2^{2+} + 2\text{H}_2\text{CO}_3 \leftrightarrow \text{UO}_2(\text{CO}_3)_2^{2-} + 4\text{H}^+$	-15.90
$\text{UO}_2^{2+} + 3\text{H}_2\text{CO}_3 \leftrightarrow \text{UO}_2(\text{CO}_3)_3^{4-} + 6\text{H}^+$	-26.45
$2\text{UO}_2^{2+} + 3\text{H}_2\text{O} + \text{H}_2\text{CO}_3 \leftrightarrow (\text{UO}_2)_2\text{CO}_3(\text{OH})_3^- + 5\text{H}^+$	-18.07

Chapter 5. Model of the uranium adsorption process onto the sediment surface

was assumed $7.74\text{m}^2/\text{g}$, because the CEC of the sediment without calcite is twice as high. Another parameter needed in the model is the density of surface sites available for uranium coordination. The value proposed by Davies and Kent (1990) of $2.31\text{ sites}/\text{nm}^2$ of surface has been used. It is an assumption of the site density for all iron oxides [21, 80]. Previously, this value has already been used by El Aamrani et al. (2002), Zavarin and Bruton (1999), Missana et al. (2003). Thus, the only additional fitting parameters are the surface complexation constants. For all cases the concentrations of $[\text{Na}^+]=0.1\text{M}$ and $[\text{NO}_3^-]=0.1\text{M}$ were also added to the model. Because the uranium spike (in the experiments) was in HNO_3 matrix, which was neutralized with NaOH . This fact is important because Na content affects uranium sorption at low pH [52].

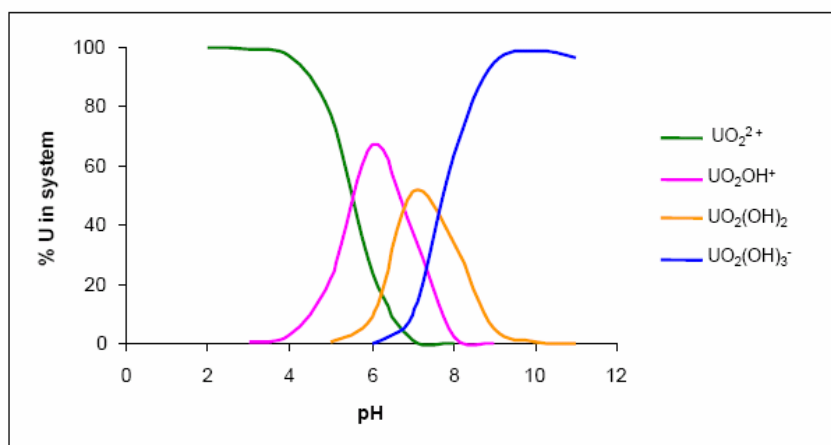


Figure 5.1. Aqueous speciation of uranium with the thermodynamic data of Table 5.1, $I= 0.1\text{M}$, $C_U= 8 \cdot 10^{-14}\text{ M}$

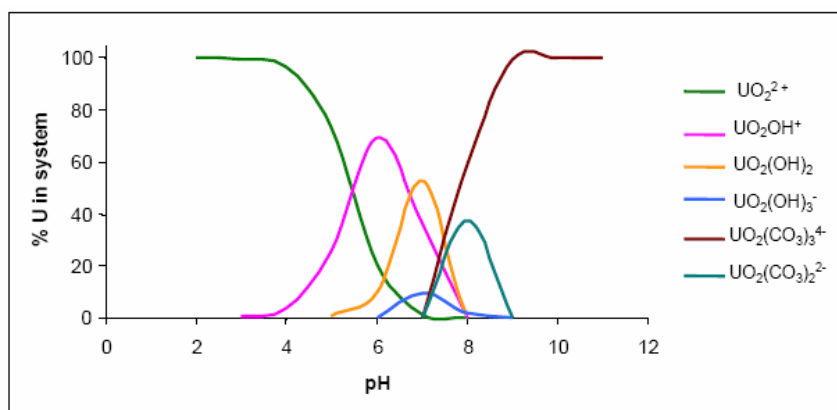


Figure 5.2. Aqueous speciation of uranium with the thermodynamic data of Table 5.1, $I=0.1\text{M}$, $C_U= 8 \cdot 10^{-14}\text{ M}$, and concentration of $\text{CaCO}_3 10^{-4}\text{M}$

Chapter 5. Model of the uranium adsorption process onto the sediment surface

The first calculation was carried out with constants of surface complexation reactions for ferrihydrate from Barnett et al (2002). The constants are displayed in the Table 5.2.

The model and experimental data are plotted in Figure 5.3. The results at $8 \cdot 10^{-13} \text{M}$ and $4 \cdot 10^{-13} \text{M}$ total U(VI), concentration $[\text{CO}_3^{2-}] = 6 \cdot 10^{-5} \text{M}$, concentration $[\text{Ca}^{2+}] = 10^{-4} \text{M}$ (concentrations were taken with the assumption that calcite is dissolved as much as possible), $\log PCO_2 = -3.5$, and $I = 0.01 \text{ M}$ indicate that the model was able to predict the major features of pH-dependent adsorption: the sharp increase in adsorption from pH 5 to pH 7 and the decrease in adsorption from pH 8 to pH 9. Although the model did predict the general trends, there were some specific differences. The major discrepancy between the model and the experimental data is seen at pH range between 7 and 10.

Table 5.2. Surface Complexation Reactions and constants for the first calculation

Surface Complexation Reactions	LogK
$\text{SOH} + \text{H}^+ \leftrightarrow \text{SOH}_2^+$	+6.51*
$\text{SOH} \leftrightarrow >\text{SO}^- + \text{H}^+$	-9.13*
U(VI) Surface Complexation Reactions	
$2 \text{SOH} + \text{UO}_2^{2+} \leftrightarrow (\text{SO})_2\text{UO}_2^0 + 2 \text{H}^+$	-3.37 ^b
$2 \text{SOH} + \text{UO}_2^{2+} + \text{H}_2\text{CO}_3 \leftrightarrow (\text{SO})_2\text{UO}_2\text{CO}_3^{2-} + 4 \text{H}^+$	-12.34*

* from Barnett et al.2000

^b from Arnold et al. 1996

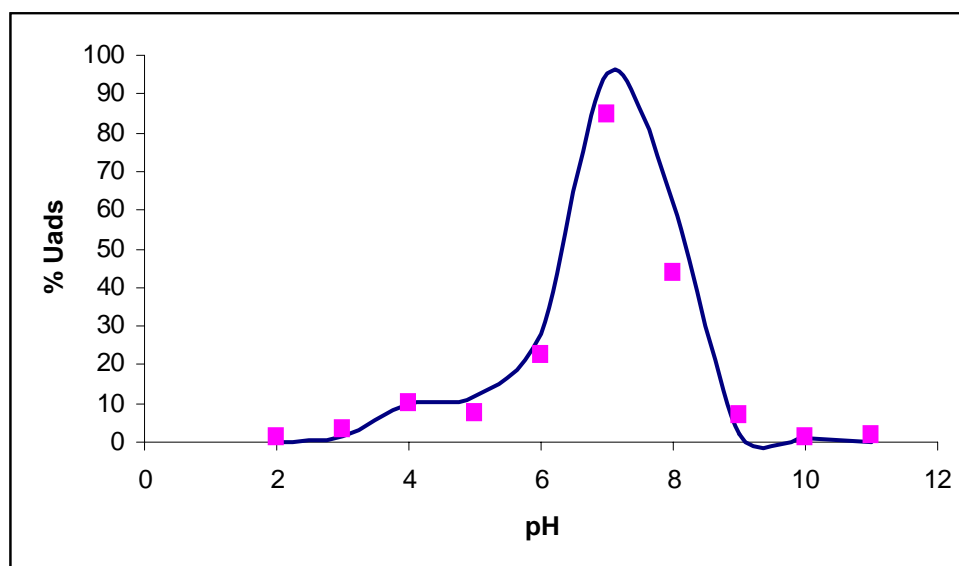


Figure 5.3. Adsorption of uranium at $[\text{CO}_3^{2-}] = 6 \cdot 10^{-5} \text{M}$. The solid line represents the model-predicted adsorption with reactions from Table 5.2; the square points – experimental data

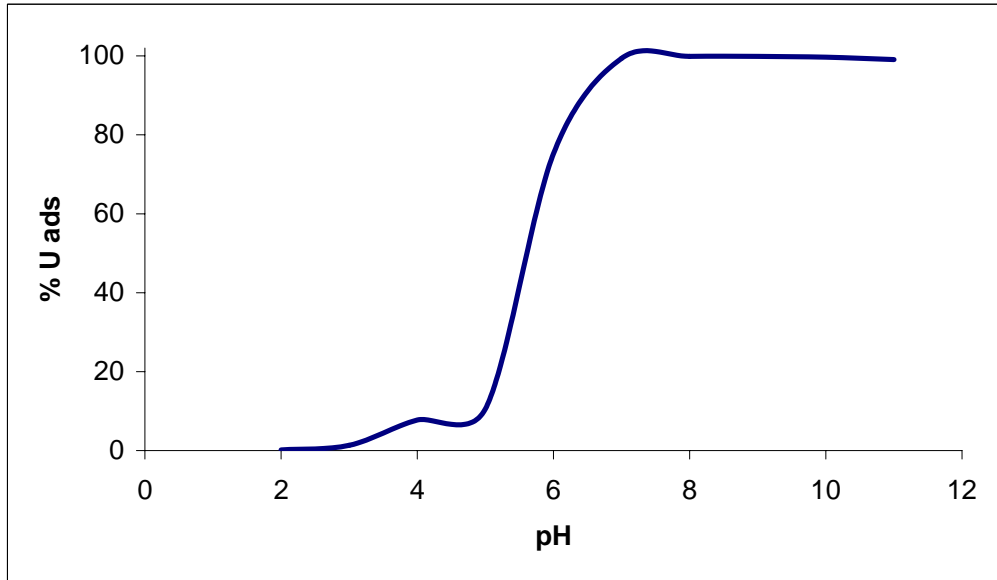


Figure 5.4. The model of uranium adsorption at $[\text{CO}_3^{2-}] = 10^{-11}\text{M}$, with reaction constants from Table 5.2

However, the model could not predict sorption difference for the cases $8 \cdot 10^{-13}\text{M}$ and $4 \cdot 10^{-13}\text{M}$ total U(VI) in the initial solution which was observed in laboratory experiments (see Chapter 4 *Results*). That can be explained due to too low uranium concentration.

The simulation of the uranium sorption in the sediment without calcite was carried out using the same surface complexation constants. The results at $8 \cdot 10^{-13}\text{M}$ total U(VI), $\log P\text{CO}_2 = -3.5$, and $I = 0.01\text{ M}$ concentration $[\text{CO}_3^{2-}] = 10^{-11}\text{M}$ are plotted in Figure 5.4. The concentration of CO_3^{2-} was fitted under the assumption that atmospheric $\text{CO}_2(\text{g})$ is dissolved in water.

This model predicted an increase of uranium sorption in the pH range between 5-7 and no decrease of uranium sorption at high pH range. However, the experimental data have shown the decrease of uranium sorption at high pH (see Chapter 4).

To produce the best fit of the model to the experimental data for sediment without calcite the author has estimated the surface complexation constants. The constants were found by trying to minimize the RMSE (Root Mean Square Error):

$$\text{RMSE} = \left[\frac{1}{n_d} \sum_{i=1}^{n_d} \left(\frac{C - C^i}{C_0} \right)^2 \right]^{1/2}$$

Chapter 5. Model of the uranium adsorption process onto the sediment surface

Table 5.3. Surface Complexation Reactions and constants which gave the best fit

Surface Acidity Reactions	LogK
$\text{SOH} + \text{H}^+ \leftrightarrow \text{SOH}_2^+$	+3
$\text{SOH} \leftrightarrow >\text{SO}^- + \text{H}^+$	-10
U(VI) Surface Complexation Reactions	
$2 \text{SOH} + \text{UO}_2^{2+} \leftrightarrow (\text{SO})_2\text{UO}_2^0 + 2 \text{H}^+$	6.28*
$2 \text{SOH} + \text{UO}_2^{2+} + \text{H}_2\text{CO}_3 \leftrightarrow (\text{SO})_2\text{UO}_2\text{CO}_3^{2-} + 4 \text{H}^+$	-16.47

*from Barnett et al.2000

where n_d is the numbers of data points, i is an index, C is measured uranium concentration, C^i is the predicted uranium concentration, and C_0 is initial uranium concentration. The RMSE is a measure of the error between the predicted and the measured values expressed as a fraction of the initial concentration (e.g., the smaller the RMSE, the better the fit of the model to the data) [6].

The sets of constants used for the modelling options, which gave the best fit, considering the whole of the experimental data, are summarized in Table 5.3.

For comparison, the surface acidity and U(VI) Surface Complexation constants, which have been used in other researches, are summarized in Table 5.4.

Figure 5.5 shows the simulation of the isotherms at 8×10^{-13} M total U(VI), $\log P\text{CO}_2 = -3.5$, concentration $[\text{CO}_3^{2-}] = 10^{-11}$ M and $I = 0.01$ M. The best fit of model was achieved under the assumption that CO_2 is dissolved in water.

The maximum U(VI) adsorbed and the pH of the second pH edge decreased, however, after a decrease in adsorption amount from pH 7 to pH 9.5, the second sorption edge reversed and began to increase again. The model predicted these effects.

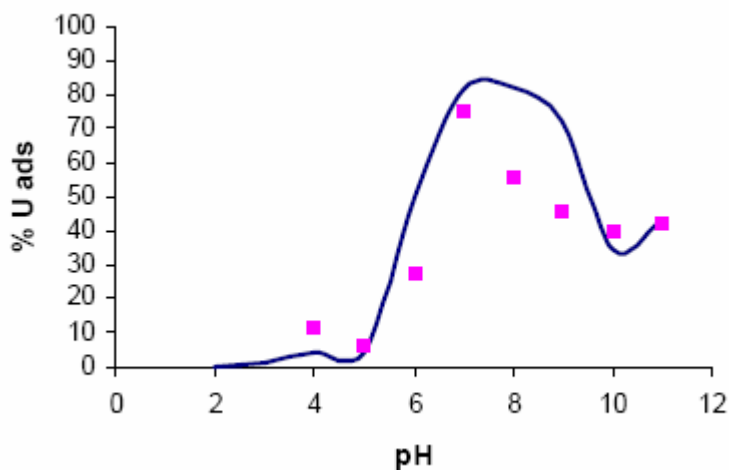
The result of calculation adsorption isotherm with using constants from Table 5.3 with calcite content (at 8×10^{-13} M total U(VI), concentration $[\text{CO}_3^{2-}] = 6 \times 10^{-5}$ M, concentration $[\text{Ca}^{2+}] = 10^{-4}$ M) is plotted on the Figure 5.6. Comparing with Figure 5.4 (isotherm plotted at the same initial conditions) the constants of surface complexation reactions from Table 5.3 gave the best fit.

Chapter 5. Model of the uranium adsorption process onto the sediment surface

Table 5.4. Surface acidity and U(VI) surface complexation constants from different studies

	LogK				
	El Aamrani et al. (2002) for olivine-rock	Missana et al. (2003) for goethite	Missana et al. (2003) for magnetite	Barnett et al.(2002), for soil	This study
Surface Acidity Reactions:					
$\text{SOH} + \text{H}^+ \leftrightarrow \text{SOH}_2^+$	3	7.2	5.2	6.51	3
$\text{SOH} \leftrightarrow >\text{SO}^- + \text{H}^+$	-10	-10	-9.1	-9.13	-10
U(VI) Surface Complexation Reactions:					
Bidentate binding					
$2 \text{SOH} + \text{UO}_2^{2+} \leftrightarrow (\text{SO})_2\text{UO}_2^0 + 2 \text{H}^+$		0.4	1.32	-6.28; -2.57	6.28
$2 \text{SOH} + \text{UO}_2^{2+} + \text{H}_2\text{CO}_3 \leftrightarrow (\text{SO})_2\text{UO}_2\text{CO}_3^{2-} + 4 \text{H}^+$				-16.43; -12.34	-16.47
Monodentate binding					
$\text{SOH} + \text{UO}_2^{2+} \leftrightarrow \text{SOUO}_2^+ + \text{H}^+$	2.4	2.8	-0.1		
$\text{SOH} + \text{UO}_2^{2+} + \text{H}_2\text{O} \leftrightarrow \text{SOUO}_2\text{OH} + 2 \text{H}^+$	-5.4	-3.7	-5.4		

(a)



(b)

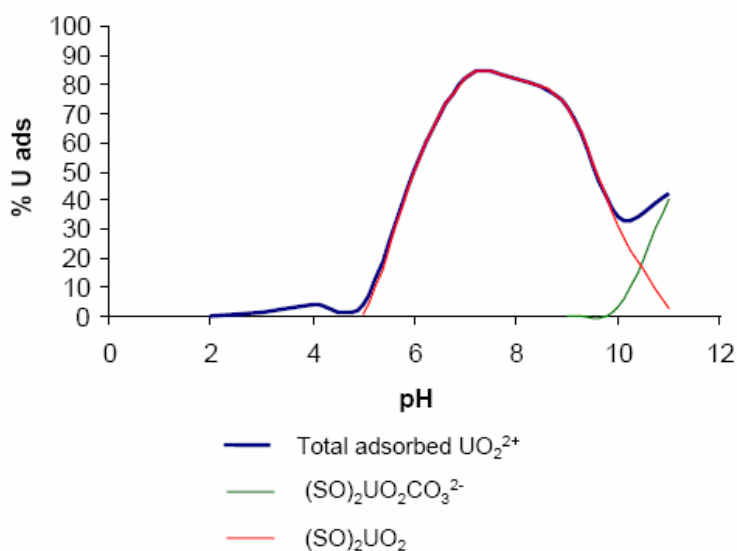


Figure 5.5 (a) Adsorption of uranium at $[\text{CO}_3^{2-}] = 10^{-11}\text{M}$. The solid line represents the model-predicted adsorption with reactions from Table 5.3, the square points – experimental data. RMSE between the model predicted values and experimental data was 0.08752

(b) Modeled U(VI) speciation: adsorbed species (red and green) and total adsorbed concentration (blue line)

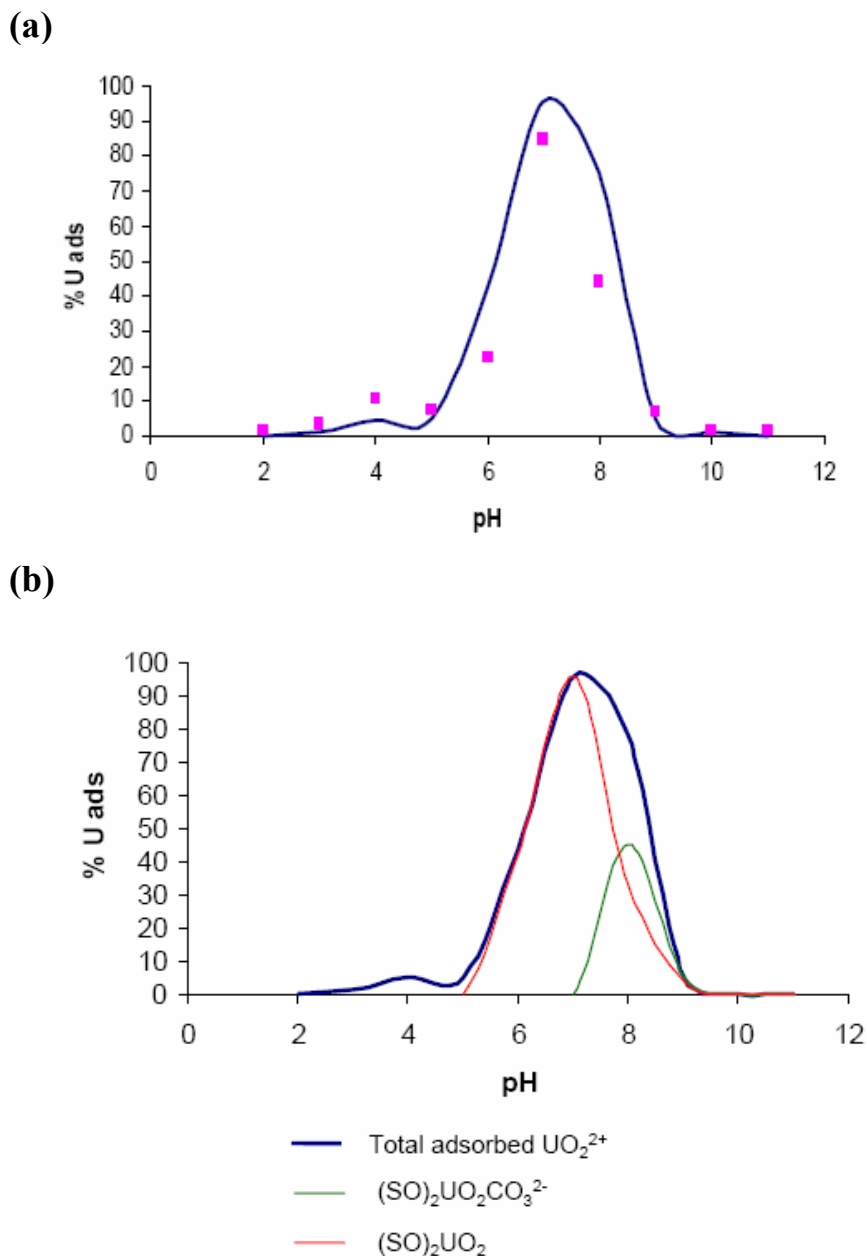


Figure 5.6. (a) Adsorption of uranium at $[\text{CO}_3^{2-}] = 10^{-4}\text{M}$. The solid line represents the model-predicted adsorption with reactions from Table 5.3, the square points – experimental data. RMSE between the model predicted values and experimental data was 0.035756

(b) Modeled U(VI) speciation: adsorbed species (red and green) and total adsorbed concentration (blue line)

5.2. Summary

The simple model for simulation of the experimental data was conducted using Visual MINTEQ 2.31.

The results shown in Figures 5.3-5.6 indicate that the surface complexation model can provide significant a priori information on the interaction of U(VI) with polycomponents media such as lake sediment. The model could predict whether U(VI) would be relatively weakly or strongly adsorbed and therefore relatively mobile or immobile in the subsurface. These results also show the profound and sometimes unexpected effects that pH and carbonate can have on U(VI) adsorption.

The Model can explain the uranium sorption behaviour at pH range between 2 and 6. The different variations of solution compound have shown that content of sodium ion in the solution decreases the uranium adsorption at pH 4-6. That has already been observed by Pabalan and Turner (1997).

The sets of surface complexation reaction constants which gave the best fit for both cases (1. natural sediment, 2. sediment without calcite) were found using RMSE method. These constants differ from the constants for ferrihydrate, which were used by Barnett et al (2002) for modelling uranium sorption. This can be explained by the fact that the observed lake sediments are a polymineral system with more than one (ferrihydrate) type of mineral surfaces. The model can well describe the properties of uranium sorption onto the sediment surface. The gained results of the model are well comparable with the results of the experimental data. This brings us to the conclusion that the model can predict uranium sorption behaviour at different carbonate concentrations.

Conclusions

The literature review shows that uranium is generally mobile in the natural environment, but it can be immobilized due to different processes, too. The important processes of uranium immobilization are uranium reduction from U(VI) to U(IV), uranium adsorption and uranium co-precipitation. For carbonates recent evidences suggest that incorporation into solid phase (co-precipitation) is the dominant uptake.

Lake Willersinnweiher is an example for redox conditions in natural environments. The uranium concentration is high in both, sediment- and water-column. Uranium from the water column is incorporated into the sediment by different processes in different seasons.

Laboratory simulation of the redox conditions in the sediment-water-column was conducted. The results show that uranium from the water column accumulates in the sediment under anoxic and oxic conditions (in “winter“ and “summer” time). Under anoxic conditions uranium is fixed in the first centimetre of the sediment. Under oxic conditions uranium penetrated deeper into the sediments.

The laboratory investigation of uranium sorption processes was carried out with lake sediment samples and with aragonite at pH range between 2 and 11. It shows that U(VI) strongly sorbs onto poly-component material such as lake sediments. The uranium sorption is strongly dependent on the pH. The maximum amount of sorption is in the neutral pH range. The content of calcite in sediment at neutral pH is unimportant, but, at high pH, it decreases the uranium sorption process. With increasing pH the process of U(VI) adsorption by natural sediment decreases due to formation of aqueous anionic U(VI)-carbonate complexes. The sorption ability of these U(VI)-carbonate complexes depends on uranium concentration in the initial solution and M/V ratio: as the sorbate/ sorbent ratio increases, the adsorption edge shifts to higher pH values. The experiments S1 and S3 indicate the increase of a U(VI) sorption amount in the pH range between 9 and 11.

Desorption of uranium is low at neutral and high pH.

Uranium uptake by calcium carbonate (coral sample) is strongly pH dependent. The maximal adsorption of U(VI) is at pH 7. In the system distilled water- powdered aragonite, uptake is fast (0.3h) due to good carbonate dissolution in distilled water. However, uranium uptake by aragonite pieces needs more time. After 24 hours the U(VI) uptake reaches just 10 %, after 60 days uptake reaches 78%. Therefore, the uranium uptake must be dependent on the rate of calcium carbonate dissolution.

Uranium uptake is dependent on solution compounds. The content of Mg^{2+} in solution highly decreases the process of uranium incorporation. Magnesium is a major element of

Conclusions

seawater. The concentration of MgCl_2 in ocean water is ~ 0.05 M, at this concentration uranium uptake decreases to 40-30 %.

Computer modelling of U(VI) sorption process by sediment was conducted. This study shows that the surface complexation model DLM can predict the major three types of uranium behaviours: (1) the increase of uranium adsorption at pH range between 5 and 6.5, (2) the maximum of adsorption at nearly neutral pH and (3) the decrease of uranium adsorption between 8 and 11.

The constants of surface complexation reaction, which are calculated with RMSE give the best fit to experimental data for natural sediment and for sediment without calcite.

It has been shown that at nearly neutral pH uranium is incorporated easily into solid phase. At the natural pH range of Lake Willersinnweiher (7.5-8.3), uranium adsorption by the sediment is high and desorption is minimal. This indicates that under oxygenated condition (“Winter” time) uranium from the water column easily incorporates into the sediment and most part of uranium does not return into the water column. This confirms the creation of authigenic uranium in sediment due to adsorption from the water column.

REFERENCES

1. Arey J.S., Seaman J.C., Bertsch P.M.. *Immobilization of Uranium in Contaminated Sediments by Hydroxyapatite Addition*. Environ. Sci. Technol. 33,(1999) pp.337-342.
2. Arnold, T.; Zorn, T.; Bernhard, G.; Nitsche, H., *Sorption of uranium (VI) onto phyllite*. Chem. Geol. 151, (1998) pp.129-141.
3. Barbarand J., Carter A., Wood I., Hurford T. *Compositional and structural control of fission-track annealing in apatite*. Chemical Geology 198, (2003) pp.107– 137.
4. Bargar J., Reitmeyer R., and Davis J., *Spectroscopic confirmation of uranium(VI)-carbonato adsorption complexes on hematite*. Environmental Science & Technology 9, Vol. 33, no. 14, (1999) pp.2481-2484.
5. Bargar J.R. , Reitmeyer R.L., Fuller C.C., Redden G.D., Davis J.A., and Piana M.J. *Remediation and Reactive Transport of Uranium (VI) in Groundwaters*. Experimental progress reports 7,(1997) pp.311-315.
6. Barnett M.O., Jardine P.M., and Brooks S.C. *U(VI) adsorption to heterogeneous subsurface media: Application of a surface complexation model*. Environ. Sci. Technol., 36, (2002) pp. 937-942.
7. Barnett M. O., Jardine P. M., Brooks S. C., and Selim H. M. *Adsorption and Transport of Uranium(VI) in Subsurface Media*. Soil Science Society of America Journal, 64(3), (2000) pp.908-917.
8. Beyenal H., Sani R.K., Peyton B.M., Dohnalkova A.C., Amonette J.E., Lewandowski Z. *Uranium Immobilization by Sulfate-Reducing Biofilms*. Environ. Sci. Technol., 38, (2004) pp.2067-2074.
9. Bourdon, B., Henderson, G. M. Lundstrom, C. C and Turner S. P.. (Eds.), *Uranium-series geochemistry*. Reviews in Mineralogy & Geochemistry vol.52, Washington, DC (2003) 656p.
10. Børretzen P. & Salbu B. *Norway Geochemical Models for Sediment-Seawater Interactions*. Laboratory for Analytical Chemistry Institute for Chemistry and Biotechnology Agricultural University of Norway, (1999) 34p.
11. Bostick B. C., Fendorf S., Barnett M.O., Jardine P.M., and Brooks S.C. *Uranyl Surface Complexes Formed on Subsurface Media from DOE Facilities*. Soil Sci. Soc. Am. J., Vol. 66, (2002) pp.99-108.
12. Brooks S., Fredrickson J.K.; Carroll S.L.; Kennedy D.W.; Zachara J.M.; Plymale A.E.; Kelly S.D.; Kemner K.M.; Fendorf S.. *Inhibition of Bacterial U(VI). Reduction by Calcium*. Environ. Sci. Technol., 37, (2003) pp.1850-1858.
13. *Chemical Thermodynamics of Uranium*. Nuclear Energy Agency Organisation for Economic Co-Operation and Development.(2004) 715p.

REFERENCES

14. Chisholm-Brause C. J., Berg J. M., Matzner R. A., and Morris D.E. *Uranium(VI) Sorption Complexes on Montmorillonite as a Function of Solution Chemistry*. Journal of Colloid and Interface Science 233, (2001) pp.38–49.
15. Christopher H. Gammons, Scott A. Wood, James P. Jonas, James P. Madison *Geochemistry of the rare-earth elements and uranium in the acidic Berkeley Pit lake, Butte, Montana*. Chemical Geology 198 (2003) pp.269– 288.
16. Cole J.M., Rasbury E.T., Montanez I.P., Pedone V.A., Lanzirrotta. And Hanson G.N. *Petrographic and trace element analysis of uranium-rich tufa calcite, middle Miocene Barstow Formation, California, USA*. Sedimentology (2004) 51, pp.433–453.
17. Duff M.C.; Amrhein C., Bertsch P.M.; Hunter D.B. *The chemistry of uranium in evaporation pond sediment in the San Joaquin Valley, California, USA, using X-ray fluorescence and XANES techniques*. Geochimica et Cosmochimica Acta. 61, 1, (1997) pp.73-81.
18. Duff M. C, Coughlin J. U., Hunter D. B. *Uranium co-precipitation with iron oxide minerals*. Geochimica et Cosmochimica Acta, Vol. 66, No. 20, (2002) pp.3533-3547.
19. Duff M., Mason C., Hunter D. *Comparison of acid and base leach for the removal of uranium from contaminated soil and catch-box media*. Canadian Journal of Soil Science. 78; 4, (1998) pp.675-683.
20. Echevarria G., Sheppard M. I., Morel J.L. *Effect of pH on the sorption of uranium in soils*. Journal of Environmental Radioactivity 53, (2001) pp.257-264.
21. El Aamrani F.Z.; Duro L.; De Pablo J.; Bruno J. *Experimental study and modeling of the sorption of uranium(VI) onto olivine-rock*. Applied Geochemistry. 17(4), (2002) pp.399-408.
22. Elyahyaoui A., Zarki R., Chiadli A. *A method for the rapid radiochemical analysis of uranium and thorium isotopes in impure carbonates*. Applied Radiation and Isotopes 58, (2003) pp.119–124.
23. Elzinga E.J.; Tait C.D.; Reeder R.J.; Rector K.D.; Donohoe R.J.; Morris D.E. *Spectroscopic investigation of U(VI) sorption at the calcite-water interface*. Geochimica et Cosmochimica Acta. 68(11), (2004) pp.2437-2448.
24. Fowle D.A.; Fein J.B.; Martin A.M. *Experimental study of uranyl adsorption onto Bacillus subtilis*. Environ.Sci.Technol. 34, (2000) pp.3737-3741.
25. Fuller C.C., Bargar J. R., Davis J.A., Piana M.J. *Mechanisms of Uranium Interactions with Hydroxyapatite: Implications for Groundwater Remediation*. Environmental Science & Technology , Vol. 36, No. 2, (2002) pp.158-165.
26. Gammons C.H.; Wood S.A.; Jonas J.P.; Madison J.P. *Geochemistry of the rare-earth elements and uranium in the acidic Berkeley Pit lake, Butte, Montana*. Chemical Geology, 198(3-4), (2003) pp.269-288.

REFERENCES

27. Giammar E.D. and Hering J.G. Time scale for sorption-desorption and surface of uranyl on goethite. *Envir.Sci.Technol.* vol.35, 16, (2001) pp.3322-3337.
28. Greathouse J.A., O'Brien R. J., Beimes G., and Pabalan R.T. *Molecular dynamic study of aqueous uranyl interactions with quartz.* *J.Phys.Chem. B*, 106, (2002) pp.1646-1655.
29. Haas J., Dichristina T., Wade R. *Thermodynamics of U(VI) sorption onto Shewanella putrefaciens.* *Chemical Geology.* 180, 1-4, (2001) pp.33-54.
30. Hennig C., Reich T., Dähn R. and Scheidegger A. M. *Structure of uranium sorption complexes at montmorillonite edge sites.* *Radiochim. Acta* 90, (2002) pp.653–657.
31. Hsi, C.-K. D.; Langmuir, D. *Adsorption of uranyl onto ferric oxyhydroxides; application of the surface complexation site-binding model.* *Geochim. Cosmochim. Acta*, 49, (1985) pp.1931-1941.
32. Hudson E., Terminello L., Viani B., Denecke M., Reich T., Allen P., Bucher J., Shuh D., Edelstein N. *The structure of U (super 6+) sorption complexes on vermiculite and hydrobiotite.* *Clays and Clay Minerals.* 47, 4, (1999) pp.439-457.
33. *Hydrogeologische Kartierung und Grundwasserbewirtschaftung Rhein-Neckar-Raum Fortschreibung 1983-1998.* Ministerium für Umwelt und Verkehr Baden-Württemberg, Hessisches Ministerium für Umwelt, Landwirtschaft und Forsten, Ministerium für Umwelt und Forsten Rheinland-Pfalz, Stuttgart . Wiesbaden . Mainz, 1999, 155p.
34. Jerden Jr.J.L., Sinha A.K., Zelazny L. *Natural immobilization of uranium by phosphate mineralization in an oxidizing saprolite-soil profile; chemical weathering of the Coles Hill uranium deposit, Virginia.* *Chemical Geology* 199, 1-2, (2003) pp.129-157.
35. Jerden Jr.J.L., Sinha A.K. *Phosphate based immobilization of uranium in an oxidizing bedrock aquifer.* *Applied Geochemistry* 18 (2003) pp.823–843.
36. Ivanovich, M. and Harmon, R. S. *Uranium-series Disequilibrium: Applications to Earth, Marine, and Environmental Sciences.* Oxford University Press. Oxford (1992) 910p.
37. Kelly S. D., Newville M. G., Cheng L., Kemner K. M., Sutton S. R., Fenter P., Sturchio N. C., Pötl C. *Uranyl Incorporation in Natural Calcite.* *Environ. Sci. Technol.*, 37, (2003) pp.1284-1287.
38. Kelly S. D., Kemner K. M., Fein J. B., Fowle D. A., Boyanov M. I., Bunker B. A., and Yee N. *X-ray absorption fine structure determination of pH-dependent U-bacterial cell wall Interactions.* *Geochimica et Cosmochimica Acta*, Vol. 66, 22, (2002) pp.3855–3871.

REFERENCES

39. Ketterer M., Wetzel W. , Layman .R, Matisoff G, Bonniwell E. *Isotopic Studies of Sources of Uranium in Sediments of the Ashtabula River, Ohio, U.S.A.* Environ. Sci. Technol., 34, (2000) pp.966-972.
40. Kitano Yasushi and Oomori Tamotsu. The coprecipitation of uranium with calcium carbonate. Journal of the Oceanographical Society of Japan 271, (1971) pp.34-42.
41. Kohler M. , Curtis G., Meece D., Davis J. *Methods for Estimating Adsorbed Uranium(VI) and Distribution Coefficients of Contaminated Sediments.* Environ. Sci. Technol., 38, (2004) pp.240-247.
42. Laukenmann S. *Transport und Austausch redoxsensitiver Elemente zwischen Freiwasser und Sediment in einem eutrophen Hartwassersee (Willersinnweiher/Ludwigshafen), unter besonderer Berücksichtigung des geochemischen Verhaltens von Uran.* PhD Thesis; University of Heidelberg (2002).
43. Lilienfein J., Qualls R.G., Uselman S.M., Bridgham S.D. *Soil formation and organic matter accretion in a young andesitic chronosequence at Mt. Shasta.* California. Geoderma 116, (2003) pp.249– 264.
44. Lomenech C., Simoni E., Drot R., Ehrhardt J.-J., and Mielczarski J. *Sorption of uranium (VI) species on zircon: structural investigation of the solid/solution interface.* Journal of Colloid and Interface Science 261 (2003) pp.221–232.
45. Martin A.J., Crusius J., Jay McNee J., Yanful E.K. *The mobility of radium-226 and trace metals in pre-oxidized subaqueous uranium mill tailings.* Applied Geochemistry 18 (2003) pp.1095–1110.
46. McKinley, J. P.; Zachara, J. M.; Smith, S. C.; Turner, G. D. *The influence of uranyl hydrolysis and multiple site-binding reactions on adsorption of U(VI) to montmorillonite.* Clays Clay Miner., 43, (1995) pp.586-598.
47. Min G.R.; Edwards R.L.; Taylor F.W.; Recy J.; Gallup C.D.; Beck J.W. *Annual cycles of U/ Ca in coral skeletons and U/Ca thermometry.* Geochimica et Cosmochimica Acta. 59; 10, (1995) pp.2025-2042.
48. Missana T., Garcia-Gutierrez M., and Fernandez V. *Uranium (VI) sorption on colloidal magnetite under anoxic environment; experimental study and surface complexation modeling.* Geochimica et Cosmochimica Acta, Vol. 67, No. 14, (2003) pp.2543-2550.
49. Missana T., García-Gutiérrez M., and Maffiotte C. *Experimental and modeling study of the uranium (VI) sorption on goethite.* Journal of Colloid and Interface Science 260 (2003) pp.291–301.
50. Missina T., Maffiotte C., and García-Gutiérrez M. *Surface reactions kinetics between nanocrystalline magnetite and uranyl.* Journal of Colloid and Interface Science 261 (2003) pp.154–160.
51. *Modelling In Aquatic Chemistry.* Oecd Publications, (1997) 724p.

REFERENCES

52. Pabalan R.T, Turner D. R. *Uranium(6+) sorption on montmorillonite; experimental and surface complexation modeling study*. Aquatic Geochemistry, vol.2, no.3, (1997) pp.203-226.
53. Pike A.W.G., Hedges R.E.M., and Van calsteren P. *U- series dating of bone using the diffusion- adsorption model*. Geochimica et Cosmochimica Acta, vol.66 no.24, (2002) pp.4273-4286.
54. Porcelli D; Andersson P.S.; Wasserburg G. J.; Ingri J.; Baskaran M. *The importance of colloids and mires for the transport of uranium isotopes through the Kalix River watershed and Baltic Sea*. Geochimica et Cosmochimica Acta. 61; 19, (1997) pp.4095-4113.
55. Reeder R. J., Nugent M., Lamble G .M.,Tait C. D.and Morris D. E. *Uranyl incorporation into calcite and aragonite: XAFS and luminescence studies*. Environ. Sci. Technol., vol. 34, no. 4, (2000) pp. 638-644.
56. Reeder R.; Nugent M., Tait C., Morris D., Heald S., Beck K., HessW., Lanzirotti A., *Coprecipitation of uranium(VI) with calcite; XAFS, micro-XAS, and luminescence characterization*. Geochimica et Cosmpchimica Acta 65, 20, (2001) pp.3491-3503.
57. Reeder R.J., Nugent M., BeckK.M., and Heald S. *Micro-XRF/XAS study of uranyl incorporation on calcite 1014 growth surfaces*. Argonne National Laboratory Report ANL-00/5 (January 2001).
58. Ritherdon B.; Hughes C.R.; Curtis C.D.; Livens F.R.; Mosselmans J. F.W.; Richardson S.; Braithwaite A. *Heat-induced changes in speciation and extraction of uranium associated with sheet silicate minerals*. Applied Geochemistry 18 (2003) pp.1121–1135.
59. Schmid J. *Calcitfällung und Phosphor-Kopräzipitation im Phosphorhaushalt eines eutrophen Hartwassersees mit anoxischem Hypolimnion (Willersinnweiher, Ludwigshafen am Rhein)*. PhD Thesis; University of Heidelberg (2002).
60. Schröder H. *Saisonale Redoxfronten im Kopplungsbereich zwischen Schwefel-Eisen- und Mangankreislauf im System Seewasser – Sediment –Grundwasser des Willersinnweiher*. PhD Thesis; University of Heidelberg (2004).
61. Senko J., Istok J., . Suflita J., Krumholz L. *In-situ evidence for uranium immobilization and remobilization*. Environ. Sci. Technol., 36, (2002) pp.1491-1496.
62. Shaw, T.J., Sholkovitz, E.R., Klinkhammer, G. *Redox dynamics in the Chesapeake Bay: The effect on sediment/water uranium exchange*. Geochim. Cosmochim. Acta, 58, (1994) pp.2985-2995.
63. Soudry D., Ehrlich S., Yoffe O., Nathan Y. *Uranium oxidation state and related variations in geochemistry of phosphorites from the Negev (southern Israel)*. Chemical Geology 189 (2002) pp.213– 230.

REFERENCES

64. Steele H. M., Wright K., and Hillier I. H. *Modelling the adsorption of uranyl on the surface of goethite*. *Geochimica et Cosmochimica Acta*, Vol. 66, No. 8, (2002) pp.1305–1310.
65. Stille P., Gauthier-Lafaye F., Jensen K.A., Salah S., Bracke G., Ewing R.C., Louvat D., Million D. *REE mobility in groundwater proximate to the natural fission reactor at Bangombe' (Gabon)*. *Chemical Geology* 198 (2003) pp.289– 304.
66. Sumner M.E.(editor). *Hand Book of Soil Science*. (2000) 2048p.
67. Swart, P. K. and Hubbard, J. A. E. B. *Uranium in scleractinian coral skeletons*. *Coral Reefs* 1, (1982) pp.13-19.
68. Sylwester E.R., Hudson E.A., and Allen P.G. *The structure of uranium (VI) sorption complexes on silica, alumina, and montmorillonite*. *Geochimica et Cosmochimica Acta*, 64, no.14, (2000) pp. 2431-2438.
69. Tokunaga T.K.; Wan J.; Pena J.; Sutton S.R. Newville-M. *Hexavalent uranium diffusion into soils from concentrated acidic and alkaline solutions*. *Environ. Sci. Technol.*, 38, 11, (2004) pp.3056-3062.
70. Tome F.V., Blanco Rodriguez M.P., Lozano J.C. *Study of the representativity of uranium and thorium assays in soil and sediment samples by alpha spectrometry*. *Applied Radiation and Isotopes*, 56(2002) pp.393-398.
71. Turner, G. D.; Zachara, J. M.; McKinley, J. P.; Smith, S. C. *Surface-charge properties and UO (sub 2) (super 2+) adsorption of a subsurface smectite*. *Geochim. Cosmochim. Acta*, vol.60, no18, (1996) pp.3399-3414.
72. Villemant B., Feuillet N. *Dating open systems by the 238U-234U-230Th method: application to Quaternary reef terraces*. *Earth and Planetary Science Letters* 210 (2003) pp.105-118.
73. Vink, J. P. M. *Measurement of Heavy Metal Speciation over Redox Gradients in Natural Water-Sediment Interfaces and Implications for Uptake by Benthic Organisms*. *Environ. Sci. Technol.*, 36, (2002) pp.5130-5138.
74. Walter M., Arnold T., Reich T., Bernhard G. *Sorption of uranium(VI) onto ferric oxides in sulfate-rich acid waters*. *Environmental-Science-and-Technology* vol.37, 13, (2003) pp.2898-2904.
75. Wilson N.S.F., Cline J.S., And Amelin Y.V. *Origin, timing, and temperature of secondary calcite–silica mineral formation at Yucca Mountain, Nevada*. *Geochimica et Cosmochimica Acta*, Vol. 67, No. 6, (2003) pp.1145–1176.
76. Viollier E., Jezequel D., Michard G., Pepe M., Sarazin G., Alberic P. *Geochemical study of a crater lake (Pavin Lake, France); trace-element behaviour in the monimolimnion*. *Chemical Geology*, 125; 1-2, (1995) pp.61-72.

REFERENCES

77. Wollschläger U. *Kopplung zwischen Oberflächengewässer und Grundwasser: Modellierung und Analyse von Umweltracern*. PhD Thesis; University of Heidelberg (2003).
78. Yang J. and Volesky B. Modeling *Uranium-Proton ion exchange in biosorption*. *Environ.Sci.Technol.*, 33, (1999) pp.4079-4085.
79. Yu Ein-Fen; Liang Chih-Hung; Chen Min-Te. *Authigenic uranium in marine sediments of the Benguela Current upwelling region during the last glacial period*. *Terrestrial, Atmospheric and Oceanic Sciences*. Vol.10, no.1, (1999) pp.201-214.
80. Zavarin M., Bruton C.J. *A non-electrostatic surface complexation approach to modeling radionuclide migration: the role of iron oxides and carbonates*. Migration '99 Seventh International Conference, Incline Village, Nevada, (1999) 17p.
81. Zheng Y., Anderson R. F, van Geen A., Fleisher M.Q. *Remobilization of authigenic uranium in marine sediments by bioturbation*. *Geochimica et Cosmochimica Acta*, Vol. 66, no. 10, (2002) pp.1759–1772.
82. Zheng Y., Weinman B., Cronin T., Fleisher M.Q., Anderson.R.F. *A rapid procedure for the determination of thorium, uranium, cadmium and molybdenum in small sediment samples by inductively coupled plasma-mass spectrometry: application in Chesapeake Bay*. *Applied Geochemistry* 18 (2003) pp.539–549.
83. Zhu C. *A case against Kd-based transport models: natural attenuation at a mill tailings site*. *Computers & Geosciences* v. 29, no. 3, (2003) pp.351-359.

Acknowledgements

I thank my supervisor Augusto Mangini for giving me opportunity to do the PhD thesis in his work-group. Also I thank him for discussion and critical review of this thesis.

I thank Margot Isenbeck-Schröter for discussion and for her helpful review of the thesis.

I thank all my colleagues and friends in Heidelberg for the friendly environment and above all Thomas, Fabio and Carsten.

I thank the DFG Graduierten-Kolleg Program 273 for three years of funding.

I thank Roswitha Marioth for her help.

Thank to Thilo Bechstädt for the nice ski-trips.

Erklärung

Hiermit erkläre ich, dass ich die vorgelegte Dissertation selbst verfasst und mich dabei keiner anderen als der von mir ausdrücklich bezeichneten Quellen und Hilfen bedient habe.

Heidelberg, den

.....